



HAL
open science

An FGFR3/MYC positive feedback loop provides new opportunities for targeted therapies in bladder cancers

Mélanie Mahé, Florent Dufour, Hélène Neyret-Kahn, Aura Moreno-Vega, Claire Béraud, Mingjun Shi, Imene Hamaidi, Virginia Sánchez-Quiles, Clémentine Krucker, Marion Dorland-Galliot, et al.

► **To cite this version:**

Mélanie Mahé, Florent Dufour, Hélène Neyret-Kahn, Aura Moreno-Vega, Claire Béraud, et al.. An FGFR3/MYC positive feedback loop provides new opportunities for targeted therapies in bladder cancers. *EMBO Molecular Medicine*, 2018, 10 (4), pp.e8163. 10.15252/emmm.201708163. hal-02066552

HAL Id: hal-02066552

<https://hal.sorbonne-universite.fr/hal-02066552>

Submitted on 13 Mar 2019

HAL is a multi-disciplinary open access archive for the deposit and dissemination of scientific research documents, whether they are published or not. The documents may come from teaching and research institutions in France or abroad, or from public or private research centers.

L'archive ouverte pluridisciplinaire **HAL**, est destinée au dépôt et à la diffusion de documents scientifiques de niveau recherche, publiés ou non, émanant des établissements d'enseignement et de recherche français ou étrangers, des laboratoires publics ou privés.

SOURCE
DATATRANSPARENT
PROCESSOPEN
ACCESS

An FGFR3/MYC positive feedback loop provides new opportunities for targeted therapies in bladder cancers

Mélanie Mahe^{1,2,†}, Florent Dufour^{1,2,†}, Hélène Neyret-Kahn^{1,2}, Aura Moreno-Vega^{1,2}, Claire Beraud³, Mingjun Shi^{1,2}, Imene Hamaidi⁴, Virginia Sanchez-Quiles^{1,2}, Clementine Krucker^{1,2}, Marion Dorland-Galliot^{1,2}, Elodie Chapeaublanc^{1,2}, Remy Nicolle^{1,2}, Hervé Lang⁴, Celio Pouponnot^{5,6,7}, Thierry Massfelder⁸, François Radvanyi^{1,2} & Isabelle Bernard-Pierrot^{1,2,*} 

Abstract

FGFR3 alterations (mutations or translocation) are among the most frequent genetic events in bladder carcinoma. They lead to an aberrant activation of FGFR3 signaling, conferring an oncogenic dependence, which we studied here. We discovered a positive feedback loop, in which the activation of p38 and AKT downstream from the altered FGFR3 upregulates MYC mRNA levels and stabilizes MYC protein, respectively, leading to the accumulation of MYC, which directly upregulates FGFR3 expression by binding to active enhancers upstream from FGFR3. Disruption of this FGFR3/MYC loop in bladder cancer cell lines by treatment with FGFR3, p38, AKT, or BET bromodomain inhibitors (JQ1) preventing MYC transcription decreased cell viability *in vitro* and tumor growth *in vivo*. A relevance of this loop to human bladder tumors was supported by the positive correlation between FGFR3 and MYC levels in tumors bearing FGFR3 mutations, and the decrease in FGFR3 and MYC levels following anti-FGFR treatment in a PDX model bearing an FGFR3 mutation. These findings open up new possibilities for the treatment of bladder tumors displaying aberrant FGFR3 activation.

Keywords BET inhibitors; bladder cancer; FGFR3; MYC; p38

Subject Categories Cancer; Urogenital System

DOI 10.15252/emmm.201708163 | Received 15 June 2017 | Revised 19 January 2018 | Accepted 23 January 2018 | Published online 20 February 2018

EMBO Mol Med (2018) 10: e8163

Introduction

Bladder cancer is the ninth most common cancer worldwide, with approximately 430,000 new cases diagnosed in 2012 and 165,000 deaths annually (Antoni *et al*, 2017). Non-muscle-invasive carcinomas (NMIBCs) account for 70% of cases at first diagnosis. These tumors often have a favorable prognosis following transurethral resection with or without intravesical chemotherapy or immunotherapy with Bacillus Calmette-Guérin (BCG). NMIBC often recurs (50–60% of cases) and sometimes progresses to a muscle-invasive tumor (5–40% progression, depending on clinical and pathological features). This high recurrence rate and the need for monitoring contribute to the economic burden of bladder cancer treatment. Muscle-invasive bladder carcinoma (MIBC) is a major clinical issue, because, even with radical cystectomy as the standard treatment, overall survival at 5 years is only about 50%, and the combination of this treatment with neoadjuvant and/or adjuvant chemotherapy increases overall survival only moderately. No major improvement in survival has been achieved over the last 20 years (Witjes *et al*, 2013). A clinical response to immune checkpoint inhibitors has recently been reported, but only a subset of patients respond to such treatment, and it remains unclear how to identify these patients (Powles *et al*, 2014; Bajorin *et al*, 2015; Bellmunt *et al*, 2017a,b; Davarpanah *et al*, 2017). Some targeted therapies have also yielded promising efficacy results. This is the case, for example, for mTOR inhibitors for patients with TSC1 mutations, anti-HER2 treatments for HER2-amplified MIBC, and anti-FGFR therapies for MIBC with activating FGFR mutations or translocations (Abbosh *et al*, 2015; Rouanne *et al*, 2016). The definition of

1 Institut Curie, CNRS, UMR144, Equipe Labellisée Ligue contre le Cancer, PSL Research University, Paris, France

2 CNRS, UMR144, Sorbonne Universités, UPMC Université Paris 06, Paris, France

3 UROLEAD SAS, School of Medicine, Strasbourg, France

4 Department of Urology, Nouvel Hôpital Civil, Hôpitaux Universitaires de Strasbourg, Strasbourg, France

5 Institut Curie, Orsay, France

6 CNRS UMR3347, Centre Universitaire, Orsay, France

7 INSERM U1021, Centre Universitaire, Orsay, France

8 INSERM UMR_S1113, Section of Cell Signaling and Communication in Kidney and Prostate Cancer, School of Medicine, Fédération de Médecine Translationnelle de Strasbourg (FMTS), INSERM and University of Strasbourg, Strasbourg, France

*Corresponding author. Tel: +33 1 42 34 63 40; Fax: +33 1 42 34 63 49; E-mail: isabelle.bernard-pierrot@curie.fr

†These authors contributed equally to this work

therapeutic strategies to improve treatment outcomes remains of the utmost importance.

FGFR3 (fibroblast growth factor receptor) belongs to a family of structurally related tyrosine kinase receptors (FGFR1-4). These receptors regulate various physiological processes, including proliferation, differentiation, migration, and apoptosis. There has been considerable interest in the FGFR family (FGFR1-4), as these receptors are frequently involved, through various mechanisms, in genetic disorders and cancer, leading to their identification as possible targets for treatment (Haugsten *et al*, 2010). *FGFR3* is frequently altered through activating mutations and translocations generating *FGFR3*-gene fusions (Billerey *et al*, 2001; Tcga, 2014). Mutations are, by far, the most frequent alterations of *FGFR3*, occurring in almost 50% of bladder tumors (70% of NMIBCs and 15–20% of MIBCs). The two most frequent mutations are the S249C and Y375C mutations, which affect the extracellular domain of the receptor. *FGFR3* translocations leading to the production of *FGFR3-TACC3* and *FGFR3-BAIAP2L1* fusion proteins were recently identified in 3% of MIBCs (Tcga, 2014). These alterations are thought to be “oncogenic drivers”, because the expression of an altered *FGFR3* induces cell transformation (Bernard-Pierrot *et al*, 2006; Williams *et al*, 2013; Wu *et al*, 2013; Nakanishi *et al*, 2015). Furthermore, several preclinical studies in cell lines and xenograft models of bladder cancer have shown that *FGFR3* alterations confer sensitivity to *FGFR* inhibitors, which have anti-proliferative and pro-apoptotic effects (Bernard-Pierrot *et al*, 2006; Wu *et al*, 2013; Nakanishi *et al*, 2015). Together, these findings highlight the critical role of *FGFR3* in bladder tumor carcinogenesis, raising the possibility of developing anti-*FGFR3* therapies for both NMIBC and MIBC (Chae *et al*, 2017). Promising results were recently reported for four out of the five patients with *FGFR3*-mutated bladder cancers enrolled in a phase I clinical trial of the pan-*FGFR* kinase inhibitor BGJ398 (Nogova *et al*, 2017). However, based on observations for other targeted therapies (EGFR, BRAF, KIT) for various cancers, including colon and lung cancers, melanoma, and gastrointestinal tumors, *FGFR3*-targeted therapies will probably turn out to be limited by multiple mechanisms of intrinsic and acquired resistance, such as ERBB2/3 or EGFR activation (Flaherty *et al*, 2012; Herrera-Abreu *et al*, 2013; Niederst & Engelman, 2013; Wang *et al*, 2015). The signaling pathway activated by mutated *FGFR3* and *FGFR3*-fusion proteins is not well characterized, particularly for bladder cancer. Improvements in our understanding of the molecular mechanisms underlying the oncogenic activity of activated *FGFR3* in bladder tumors may facilitate the identification of new drug targets that could be acted on together with *FGFR3*, to increase the efficacy of anti-*FGFR3* therapies and/or to prevent potential drug resistance. Such strategies, based on the simultaneous inhibition of two or more targets in a single pathway, have already been explored for many specific pairs of agents, in both clinical and preclinical studies (Flaherty *et al*, 2012; Li *et al*, 2014; Ran *et al*, 2015). In this study, we aimed to characterize the aberrantly activated *FGFR3* signaling pathways involved in bladder cancer cell growth/transformation. We studied genes regulated by constitutively activated *FGFR3* in two bladder tumor-derived cell lines, MGH-U3 and RT112, harboring an *FGFR3* mutation (Y375C) and a fusion gene (*FGFR3-TACC3*), respectively. We identified *MYC* as a key transcription factor that is overexpressed and activated in response to *FGFR3* activity, and critical for *FGFR3*-induced cell proliferation. We showed here that

FGFR3 is a direct target gene of *MYC*, which binds to active enhancers located upstream from *FGFR3*, establishing an *FGFR3/MYC* positive feedback loop. This loop may be relevant in human tumors, because *MYC* and *FGFR3* expression levels were found to be positively correlated in tumors bearing *FGFR3* mutations in two independent transcriptomic datasets ($n = 63$ and $n = 271$), and because *FGFR3* inhibition in a patient-derived tumor xenograft (PDX) model harboring an *FGFR3-S249C* mutation decreased the levels of both *MYC* and *FGFR3*. We found that *MYC* mRNA levels and protein stability were dependent on p38 and AKT activation, respectively, downstream from *FGFR3* activation. Finally, we showed, in xenograft models, that *FGFR3* activation conferred sensitivity to *FGFR3* and p38 inhibitors and to a BET bromodomain inhibitor (JQ1) preventing *MYC* transcription. These findings therefore suggest new treatment options for bladder cancers in which *FGFR3* is aberrantly activated.

Results

MYC is a key master regulator of proliferation in the aberrantly activated *FGFR3* pathway

We investigated the molecular mechanisms underlying the oncogenic activity of aberrantly activated *FGFR3* in bladder carcinomas, by studying the MGH-U3 and RT112 cell lines. These cell lines were derived from human bladder tumors, and they endogenously express a mutated activated form of *FGFR3* (*FGFR3-Y375C*, the second most frequent mutation in bladder tumors) and the *FGFR3-TACC3* fusion protein (the most frequent *FGFR3* fusion protein in bladder tumors), respectively. The growth and transformation of these cell lines are dependent on *FGFR3* activity (Bernard-Pierrot *et al*, 2006; Williams *et al*, 2013; Wu *et al*, 2013). We conducted a gene expression analysis with Affymetrix DNA arrays, in these cell lines, with and without *FGFR3* siRNA treatment. We identified 741 and 3,124 genes displaying significant differential expression after *FGFR3* depletion in MGH-U3 and RT112 cells, respectively (adjusted P -values < 0.05 , $|\log_2(\text{FC})| > 0.5$; Dataset EV1). An analysis of these two lists of *FGFR3*-regulated genes using the upstream regulator function of Ingenuity Pathway Analysis (IPA) software identified upstream regulators activated and inhibited by *FGFR3* (Fig 1A, left panel). The top 10 transcriptional regulators with activity modulated by *FGFR3* were common to the two cell lines and are listed in the right panel in Fig 1A. The transcription factor predicted to be the most strongly inhibited here after *FGFR3* depletion, in both cell lines, was the proto-oncogene *MYC*, for which mRNA levels were downregulated. This downregulation of *MYC* mRNA levels after *FGFR3* knockdown with siRNA was further confirmed by reverse transcription-quantitative polymerase chain reaction (RT-qPCR) (30–70% decrease, depending on the cell line used; Fig 1B). Consistent with these results suggesting that *MYC* mRNA levels are modulated by constitutively activated *FGFR3*, an analysis of previously described transcriptomic data for our CIT-series (“*Carte d’Identité des Tumeurs*”; tumor identity card) of bladder tumors revealed a significant upregulation of *MYC* mRNA levels in tumors harboring an *FGFR3* mutation ($n = 63$) relative to normal urothelium samples ($n = 4$), whereas no such overexpression was observed for tumors expressing wild-type *FGFR3* ($n = 122$; Fig 1C). Moreover, *MYC*

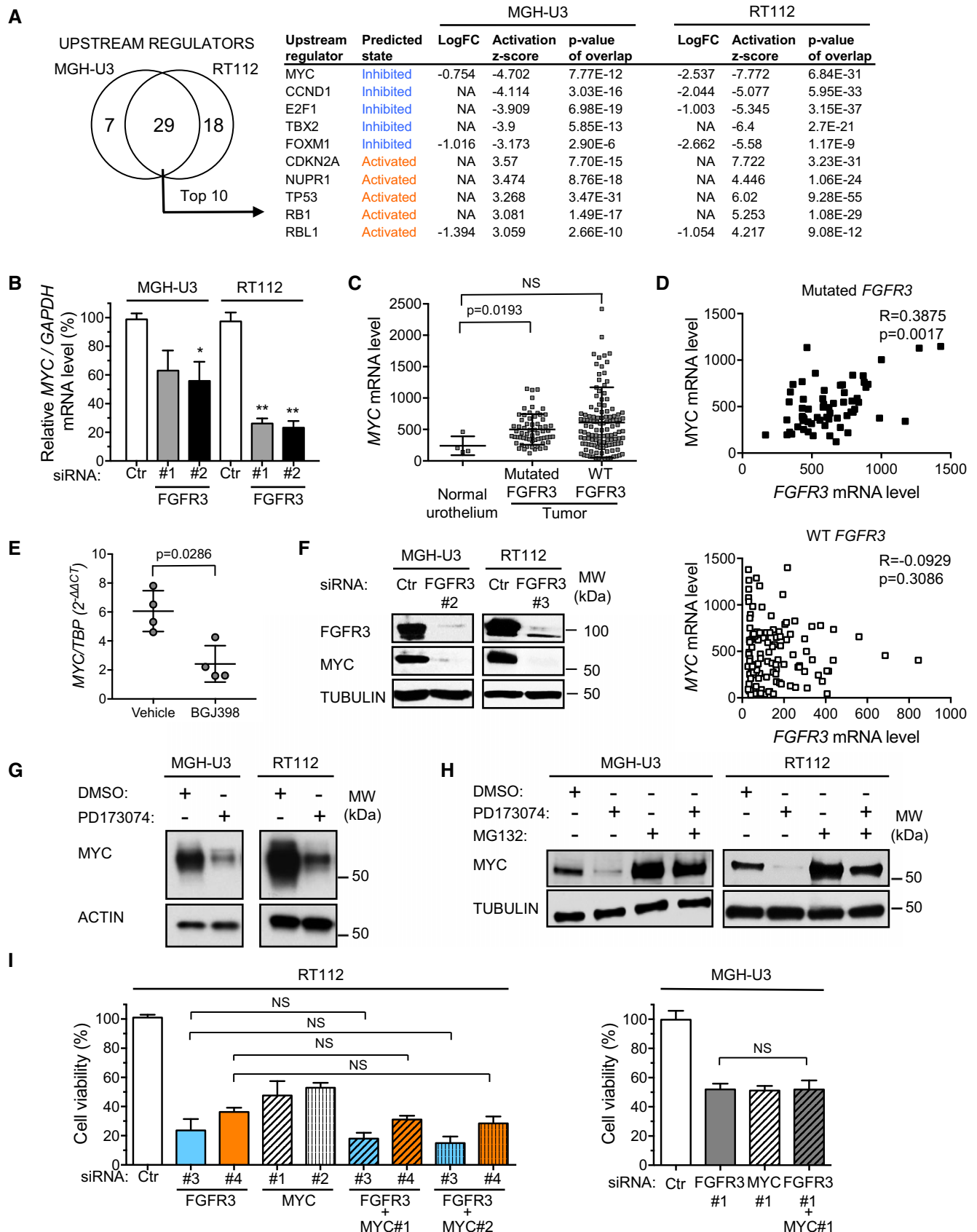


Figure 1.

Figure 1. MYC is a key upstream regulator activated by FGFR3 that is required for FGFR3-induced bladder cancer cell growth.

- A Venn diagram showing the number of upstream regulators (transcription factors) significantly predicted by Ingenuity Pathway Analysis to be involved in the regulation of gene expression observed after *FGFR3* knockdown in RT112 and MGH-U3 cells (left panel). List of the top 10 upstream regulators modulated by *FGFR3* expression in both cell lines. The Log_2FC of the transcription factor itself is also indicated. NA indicates that the FC was beyond the threshold defining genes as differentially expressed after *FGFR3* depletion (see Materials and Methods).
- B Relative *MYC* mRNA levels in MGH-U3 and RT112 cells transfected for 72 h with siRNAs targeting *FGFR3* or a control siRNA (Ctr). The results presented are the means of two independent experiments carried out in triplicate; the standard errors are indicated. The significance of differences was assessed in unpaired Student's *t*-tests, * $P < 0.05$; ** $0.001 < P < 0.005$.
- C *MYC* mRNA levels in normal human urothelium ($n = 4$) and in the CIT cohort of human bladder tumors bearing *FGFR3* mutations ($n = 63$) or wild-type *FGFR3* ($n = 122$). The significance of differences was assessed in Mann–Whitney tests, and means and standard errors are represented.
- D *MYC* and *FGFR3* mRNA levels in human bladder tumors harboring either mutated *FGFR3* (upper panel) or wild-type *FGFR3* (lower panel). Spearman's coefficient and *P*-values are indicated for the correlations between *MYC* and *FGFR3* mRNA levels in each group.
- E *MYC* mRNA levels in a PDX model bearing a *FGFR3*-S249C mutation and treated daily, for 4 days, with 30 mg/kg BGJ398, a pan-FGFR inhibitor, or with vehicle ($n = 4$ mice per group). Means and standard errors are represented. The significance of differences was assessed in Mann–Whitney tests.
- F Western blot (72 h after transfection) comparing *FGFR3* and *MYC* levels in MGH-U3 and RT112 cells transfected with a control siRNA (Ctr) or with siRNAs targeting *FGFR3*.
- G Western blot comparing *MYC* levels in MGH-U3 and RT112 cells, treated for 2 h with DMSO or the pan-FGFR inhibitor, PD173074 (500 nM).
- H Western blot comparing *MYC* levels in MGH-U3 and RT112 cells treated for 3 h with FGFR inhibitor (0.5 μM PD173074) or proteasome inhibitor (10 μM MG132), alone or in combination.
- I Cell viability assay comparing the impact of *MYC* and/or *FGFR3* downregulation on RT112 (left panel, CellTiter-Glo) and MGH-U3 (right panel, MTT assay) cell viability (72 h post-transfection). The results presented are the means of three independent experiments carried out in triplicate, error bars represent standard deviations. Tukey's multiple comparisons tests were performed to evaluate the significance of differences. The results of the statistical analysis are summarized in Dataset EV2.

Source data are available online for this figure.

expression was positively correlated with *FGFR3* expression in bladder tumors harboring a mutated *FGFR3* (Fig 1D, upper panel), whereas no such correlation was observed in tumors bearing wild-type *FGFR3* ($n = 122$; Fig 1D, lower panel). Similar results were also observed for another publicly available transcriptomic dataset for 416 bladder tumors (271 with *FGFR3* mutations) and eight normal samples (Hedegaard *et al*, 2016; Appendix Fig S1A and B), suggesting that mutated *FGFR3* may also regulate *MYC* expression in human bladder carcinomas. Support for this hypothesis was provided by the significant decrease in *MYC* mRNA levels induced by 4 days of anti-FGFR treatment in tumors from a PDX model (F659) bearing an *FGFR3*-S249C mutation (Fig 1E). As in cell lines, *FGFR3*-S249C expression conferred *FGFR3* dependence on the PDX model, in which anti-FGFR treatment with BGJ398 decreased tumor growth by 60% after 29 days of administration (Appendix Fig S2).

MYC is a key regulator of proliferation and its deregulation can promote oncogenesis in various types of cancer (Dang, 2012). We therefore investigated the role of *MYC* as a master regulator of proliferation in bladder cell lines expressing aberrantly activated *FGFR3*. Western blot analysis further showed that *FGFR3* depletion resulted in the almost total loss of *MYC* from both MGH-U3 and RT112 cells (Fig 1F). The discrepancy between the decreases in *MYC* mRNA (Fig 1B) and protein levels (Fig 1F) suggested that the aberrant activation of *FGFR3* regulated *MYC* not only at mRNA level, but also through stabilization of the protein. This hypothesis was also supported by the time course of *MYC* expression on Western blots after the inhibition of *FGFR3* with PD173074. Indeed, *MYC* levels decreased rapidly, after 30 min of treatment, in MGH-U3 cells (Appendix Fig S3A), and expression was totally lost after 2 h of treatment, in both MGH-U3 and RT112 cells (Fig 1G and Appendix Fig S3A). *MYC* protein stability is, thus, tightly controlled by the proteasome. We therefore investigated the possible role of *FGFR3* in this process, by treating MGH-U3 and RT112 cells with a pan-FGFR inhibitor (PD173074), either alone or in combination with a proteasome inhibitor (MG132; Fig 1H). Western blot analysis showed that the downregulation of *MYC* induced by the

inhibition of *FGFR3* was abolished by MG132, in both cell lines. Overall, our results indicate that the inhibition of aberrantly activated *FGFR3* decreases *MYC* mRNA levels and favors proteolysis of the *MYC* protein by the proteasome, thereby decreasing its transcriptional activity. We then investigated the possible contribution of *MYC* to the oncogenic activity of aberrantly activated *FGFR3*. We compared the effects on viability of depleting *FGFR3* and *MYC* alone or together, with siRNA, in RT112 and MGH-U3 cells (Fig 1I). *FGFR3* and *MYC* siRNAs efficiently knocked down the levels of the targeted proteins (Appendix Fig S3B). The depletion of either *MYC* or *FGFR3* resulted in significantly lower cell viability than for cells treated with the control siRNA (Fig 1I, right and left panels and Dataset EV2 for the *P*-values). No significant additive effect relative to *FGFR3* depletion alone was observed in RT112 and MGH-U3 cells with a simultaneous knockdown of *FGFR3* and *MYC* expression, suggesting that *MYC* is a key downstream effector of the aberrantly activated *FGFR3* pathway mediating cell proliferation.

FGFR3 and MYC are involved in a positive feedback loop in which FGFR3 is a direct transcriptional target of MYC in bladder cancer cell lines with constitutively activated FGFR3

Surprisingly, we observed that the treatment of MGH-U3 and RT112 cells with a *MYC* siRNA strongly decreased *FGFR3* levels (Fig 2A). RT-qPCR showed that this loss of *FGFR3* expression was due to a decrease in *FGFR3* mRNA levels after *MYC* knockdown (Fig 2B). We investigated whether *FGFR3* was a direct transcriptional target of *MYC*, by analyzing *MYC* occupancy of the *FGFR3* locus by chromatin immunoprecipitation and quantitative PCR (ChIP-qPCR). Using the publicly available ENCODE data for three different cancer cell lines, we designed primers binding to two potential enhancers, the promoter and an intragenic region of *FGFR3* (Appendix Fig S4A). According to ENCODE data, the enrichment of *MYC* and activation marks (H3K27ac) in the E1 and E2 enhancers is correlated with the level of *FGFR3* transcription (Appendix Fig S4A). We

checked, by ChIP-qPCR, that the selected FGFR3 promoter and enhancers did harbor the expected histone activation marks (H3K27ac and H3K4me3) in RT112 cells (Appendix Fig S4B). Finally, we showed that the two *FGFR3* enhancer regions tested were enriched in *MYC*, consistent with the direct regulation of *FGFR3* expression by *MYC*, at the transcriptional level (Fig 2C). This regulation of *FGFR3* by *MYC* seemed to be quite specific to bladder cancer, because *MYC* binding to the *FGFR3* enhancers or promoter was rarely observed in a publicly available dataset encompassing 118 *MYC* chromatin immunoprecipitation and sequencing (ChIP-Seq) in different tissues (Appendix Fig S5A). Binding was observed in two known FGFR3-dependent cell lines, MCF7 and HepG2 (Qiu *et al*, 2005; Tomlinson *et al*, 2012), in some blood-derived cell lines and in one lung cancer-derived cell line. *MYC* activation did not seem to be sufficient to induce FGFR3 regulation. Indeed, *MYC* ChIP-Seq data acquired for two inducible models of *MYC* overexpression/activation (LNCaP and U2OS cells; Walz *et al*, 2014; Barfeld *et al*, 2017) showed no *MYC* enrichment on the *FGFR3* enhancers or promoter after *MYC* activation (Appendix Fig S5B and C). Our data therefore identify *MYC* as a master regulator of proliferation activated downstream from FGFR3 (Fig 1) and as a positive regulator of FGFR3 expression in bladder cancer lines (Fig 2A–C). Consistent with this FGFR3/*MYC* positive feedback loop, we also observed that the treatment of RT112 and MGH-U3 cells with a pan-FGFR kinase inhibitor abolished both *MYC* and FGFR3 expression (Fig 2D). This result was confirmed in two other cell lines expressing constitutively activated FGFR3: UM-UC-14 (FGFR3-S249C) and RT4 (FGFR3-TACC3 breakpoint exon 18 FGFR3–exon 4 TACC3, whereas FGFR3-TACC3 breakpoint exon 18 FGFR3–exon 11 TACC3 is expressed in RT112; Williams *et al*, 2013; Earl *et al*, 2015; Fig 2D). These four cell lines express low levels of *FGFR1*, *FGFR2*, and *FGFR4*, as assessed with an Affymetrix U133plus2 array, suggesting that the observed effect was mostly due to FGFR3 inhibition (data not shown). However, treatment had no effect on *MYC* and FGFR3 expression in UM-UC-5 cells, which express wild-type FGFR3 (Fig 2D). These results suggest that the FGFR3/*MYC* positive feedback loop is a general mechanism, regardless of the type of FGFR3 alteration, but that it is dependent on activated FGFR3. Using RT112 and MGH-U3 xenograft models treated for 9 days with a pan-FGFR inhibitor, PD173074, which delayed tumor growth (Appendix Fig S6A), we also showed *in vivo* that FGFR3 and *MYC* were involved in a positive feedback circuit inducing bladder tumor growth. Indeed, immunoblot analysis revealed that FGFR3 inhibition resulted in lower levels of both *MYC* and FGFR3 in the xenografts (Fig 2E). Finally, we made use of our PDX model (F659) harboring an FGFR3-S249C mutation to demonstrate that this FGFR3/*MYC* loop was relevant to human tumors. Indeed, the treatment of tumor-bearing mice for 4 days with another pan-FGFR inhibitor, BGJ398, which inhibited PDX tumor growth (Appendix Fig S6B), decreased both *MYC* and FGFR3 levels in the tumors (Fig 2F).

MYC accumulation induced by aberrantly activated FGFR3 in bladder tumors depends on p38 and AKT activation

Given the importance of the FGFR3/*MYC* loop in all our tested models, including the PDX model, we characterized the underlying mechanisms. We investigated the signals downstream from FGFR3

responsible for the observed higher levels of *MYC* mRNA and greater *MYC* protein stability in bladder cancer cells harboring FGFR3 mutations (Fig 1).

We first used transformed NIH-3T3 cells expressing FGFR3-S249C established in a previous study (Bernard-Pierrot *et al*, 2006) to confirm that mutated FGFR3 expression induced an upregulation of *MYC* mRNA levels (Appendix Fig S7A). We investigated the activation of three pathways known to be activated by tyrosine kinase receptors and, in particular, FGFRs (p38, AKT, ERK1/2; Powers *et al*, 2000; Appendix Fig S7B), and evaluated their role in the cell transformation induced by mutated FGFR3 (Appendix Fig S7C). We found that the activation of p38 and AKT mediated cell transformation downstream from the mutated FGFR3 whereas ERK1/2 activation was less crucial for FGFR3 activity. It has been established that p38 can induce the stabilization of *MYC* mRNA or the upregulation of *MYC* protein levels through an increase in transcription (Chen *et al*, 2005) whereas AKT can induce the stabilization of *MYC* protein (Tsai *et al*, 2012). We thus investigated the involvement of these two pathways in our urothelial models, MGH-U3 and RT112 cells. We showed that p38 and AKT were constitutively activated in both cell lines. This activation was dependent on FGFR3 expression, because it was abolished by *FGFR3* knockdown (Fig 3A). We then explored the role of p38 in the FGFR3-induced upregulation of *MYC* mRNA levels, using a p38 siRNA targeting *MAPK14* (p38 α), the predominant isoform in MGH-U3 and RT112 cells, as shown by Affymetrix U133 plus 2.0 DNA chip analyses (data not shown). Immunoblot analysis showed that the efficient depletion of p38 resulted in the loss of about 50% of *MYC* in both MGH-U3 and RT112 cells, whereas *MYC* loss was total following *FGFR3* depletion (Fig 3B). This decrease in *MYC* levels is consistent with the decrease in *MYC* mRNA levels observed on RT-qPCR 72 h after p38 depletion (Fig 3C), suggesting that p38 plays a key role in *MYC* mRNA regulation but that another pathway downstream from FGFR3 is probably responsible for regulating the stability of the protein (Fig 1).

MYC degradation by the proteasome is regulated by glycogen synthase kinase 3 (GSK3). The activity of GSK3 is regulated by phosphorylation, including that of the Ser9 residue of GSK3 β and the Ser21 residue of GSK3 α , by AKT, in particular (Gregory *et al*, 2003). In accordance with this mechanism, we demonstrated, in RT112 and MGH-U3 cells, that FGFR3 inhibition with a pan-FGFR inhibitor (PD173074) decreased the phosphorylation of AKT at Ser473 and that of GSK3 β at Ser9 (Fig 3D). We found that PI3-kinase inhibition by LY294002 inhibited AKT phosphorylation and decreased both the phosphorylation of the Ser9 residue of GSK3 β and *MYC* protein levels (Fig 3E). Thus, FGFR3 induces AKT phosphorylation, leading to the inhibition of GSK3 β through Ser9 phosphorylation, thereby preventing the proteasome-mediated proteolysis of *MYC*. Our results thus demonstrate that, downstream from the aberrantly activated FGFR3, both p38 and AKT are involved in the induction of *MYC* accumulation, which, in turn, drives cell proliferation. Consistent with these results for p38, reverse-phase protein array (RPPA) analysis of a panel of 129 tumors showed that p38 was significantly more phosphorylated in tumors expressing a mutated FGFR3 than in tumors expressing wild-type FGFR3 (Fig 3F, left panel). AKT was not differentially phosphorylated in tumors with and without *FGFR3* mutations, suggesting that, in bladder cancer, AKT can be activated by several mechanisms including the aberrant activation of FGFR3,

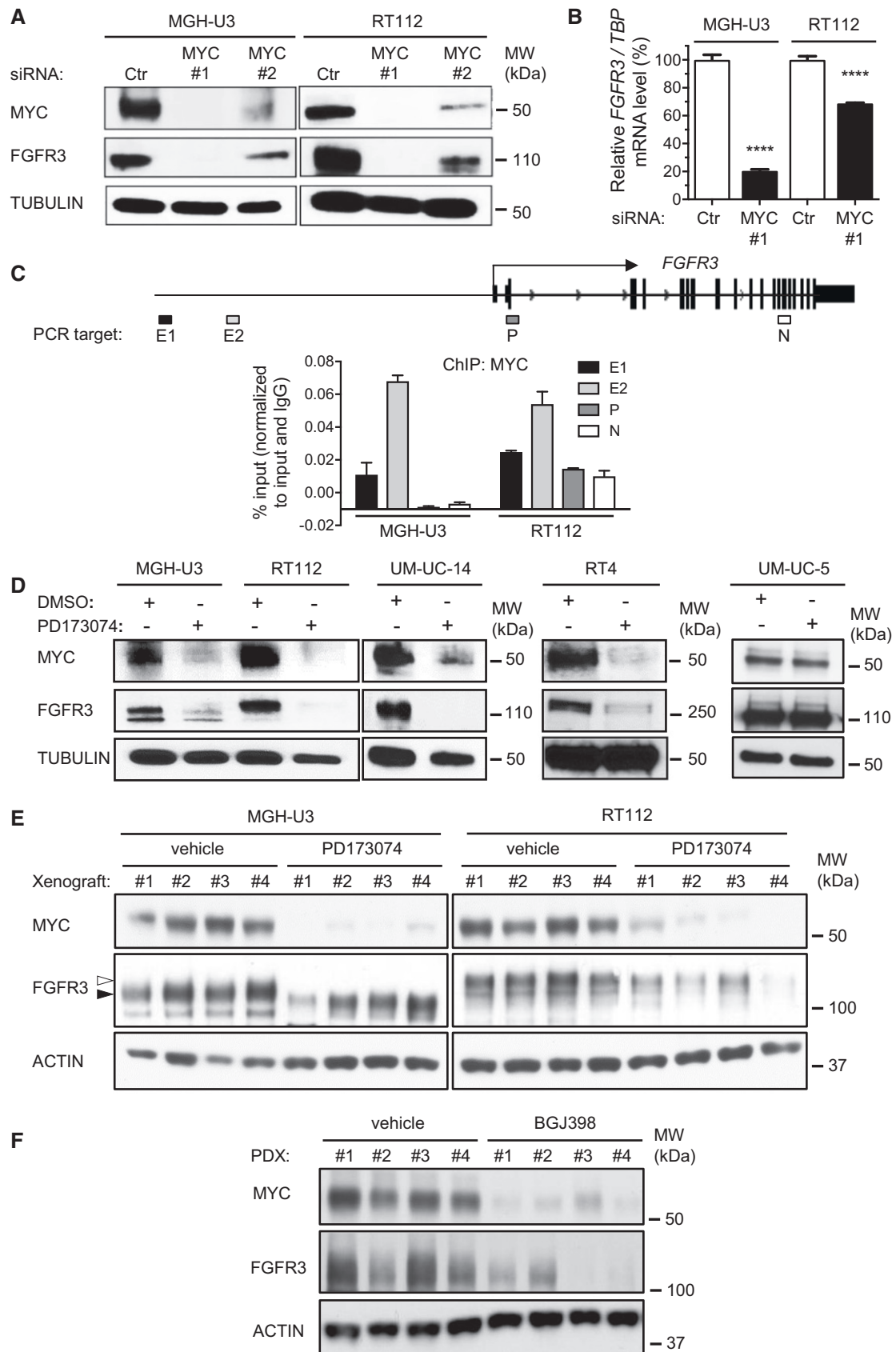


Figure 2.

Figure 2. MYC and FGFR3 are involved in a positive feedback loop in bladder cancer cell lines expressing an activated form of FGFR3.

- A The expression of MYC and FGFR3 was analyzed by Western blotting in lysates from MGH-U3 and RT112 cells transfected for 72 h with MYC siRNAs. Tubulin was used as a loading control.
- B Relative *FGFR3* mRNA levels in MGH-U3 and RT112 cells transfected for 72 h with siRNAs targeting MYC or a control siRNA (Ctr). The results presented are the means of two independent experiments carried out in triplicate; the standard errors are indicated. Unpaired Student's *t*-tests were used for comparison with the control, *****P* < 0.0001.
- C ChIP-qPCR for MYC at the *FGFR3* locus in MGH-U3 and RT112 cells (lower panel). The qPCR target loci of *FGFR3* are schematized (upper panel). Data presented are representative of two replicate experiments. Error bars show standard deviation of three replicate qPCR reactions.
- D RT112, MGH-U3, UM-UC-14, RT4, and UM-UC-5 cells were treated for 48 h with a pan-FGFR inhibitor (500 nM PD173074). Lysates were obtained, and levels of FGFR3 and MYC were analyzed by Western blotting with appropriate antibodies. An anti-tubulin antibody was used as a loading control.
- E MGH-U3 and RT112-derived xenograft tumors from mice treated for 9 days with vehicle or PD173074 (25 mg/kg/day) were lysed and immunoblotted with anti-FGFR3 and anti-MYC antibodies. Actin was used as a loading control. Black and white arrowheads indicate WT FGFR3 and FGFR3-TACC3 bands, respectively.
- F PDX tumors bearing the FGFR3-S249C mutation from mice treated for 4 days with vehicle or BGJ398 (30 mg/kg/day) were lysed and immunoblotted with anti-FGFR3 and anti-MYC antibodies. Actin was used as a loading control.

Source data are available online for this figure.

such as EGFR activation in basal tumors (Rebouissou *et al*, 2014; Fig 3F, right panel). The FGFR3/MYC positive feedback loop involving p38 and AKT activation by FGFR3 identified in bladder cancer cell lines may, therefore, also occur in human bladder tumors with genetic alterations of FGFR3. The disruption of this loop with inhibitors of AKT and p38 may, therefore, constitute an effective way of treating these tumors.

Targeting FGFR3, p38, or AKT is an effective strategy for inhibiting the growth and transformation of bladder cancer cells expressing aberrantly activated FGFR3

We evaluated the effects of p38 and PI3K inhibitors (SB203580 and LY294002, respectively) on the viability of RT112 and MGH-U3 cells (Fig 4A) and on MGH-U3 cell transformation (Fig 4B). The inhibition of these two pathways decreased the viability of MGH-U3 and RT112 cells and the anchorage-independent growth of MGH-U3 cells as efficiently as FGFR3 inhibition with a pan-FGFR inhibitor, PD173074. Using a *MAPK14* siRNA, we confirmed that p38 α depletion decreased the viability of RT112 and MGH-U3 cells and the anchorage-independent growth of MGH-U3 cells (Fig 4C and D). We also validated *in vivo* the critical role of p38 in mutated FGFR3-induced tumor growth, by showing that p38 inhibition with SB203580 significantly slowed the tumor growth of MGH-U3 and RT112 xenografts in athymic nude mice (Fig 4E). An AKT inhibitor has already been shown to decrease MGH-U3 xenograft growth slightly in athymic nude mice (Davies *et al*, 2015).

MYC acts as a key master regulator of proliferation in the FGFR3 pathway, rendering FGFR3-dependent cells sensitive to a BET bromodomain inhibitor (JQ1)

We looked for other ways to disrupt the FGFR3/MYC loop in bladder tumors bearing *FGFR3* mutations. Recent studies have shown that the indirect inhibition of MYC through the targeting of proteins involved in the regulation of its transcription is an effective strategy for treating MYC-dependent tumors (Posternak & Cole, 2016). In particular, several studies have highlighted the use of bromodomain inhibitors as an effective strategy for blocking MYC transcription (Delmore *et al*, 2011; Mertz *et al*, 2011). We therefore focused on JQ1, a potent and well-characterized BET bromodomain inhibitor that inhibits the binding of bromodomain-containing protein 4 (BRD4) to acetylated lysine residues on histones, thereby preventing

transcription. It is particularly active against MYC, the transcription of which seems to be dependent on the binding of BRD4 to its enhancers or “super-enhancers” (Lovén *et al*, 2013). We first analyzed the BRD4 occupancy of the MYC locus by ChIP-qPCR in the RT112 and MGH-U3 bladder cell lines (Fig 5A). Using publicly available data for histone marks, we designed primers binding to one potential enhancer, one control negative region and the promoter (Appendix Fig S8A) and checked that the selected regions harbored the expected histone marks in the RT112 bladder cell line (Appendix Fig S8B). The MYC enhancer was slightly enriched in BRD4, and the MYC promoter was strongly enriched in BRD4. In both cases, this enrichment was prevented by JQ1 treatment (Fig 5A). We then checked, by Western blotting, that JQ1 treatment inhibited MYC and FGFR3 expression, in both cell lines (Fig 5B). The observed inhibition was of similar strength to the FGFR3 inhibition observed with 1 μ M PD173074 (Fig 5B). By contrast, treatment with (–)-JQ1, the inactive enantiomer of (+)-JQ1, had little impact on MYC and FGFR3 levels (Fig 5B). Consistent with this inhibition of MYC and FGFR3 expression following JQ1 treatment, we also showed that JQ1 treatment significantly decreased the viability of RT112 and MGH-U3 cells *in vitro* (Fig 5C). Finally, we showed *in vivo* that JQ1 treatment significantly slowed the growth of MGH-U3 and RT112 xenografts in nude mice (Fig 5D). However, on the one hand, the inhibition of tumor growth by JQ1 treatment was relatively modest. In the other hand, although they slowed tumor growth, FGFR inhibitors did not trigger a regression of tumor size (Appendix Fig S6A). We therefore hypothesized that a combinatorial treatment might improve the response. We tested this hypothesis *in vitro*, on MGH-U3 and RT112 cell viability that made it possible to use ranges of doses for both molecules (Appendix Fig S9A). We found that simultaneous use of the two drugs increased treatment efficacy over that achieved with the two drugs used separately, as highlighted in Fig 5E. A mathematical analysis of our results by the Loewe additivity method (Fouquier & Guedj, 2015) showed that the two drugs had an additive effect in most cases, and possibly even a synergistic effect at some concentrations (Appendix Fig S9B).

Discussion

Alterations of FGFR3 (mutations or translocation) are among the most frequent genetic events in bladder carcinoma, occurring in

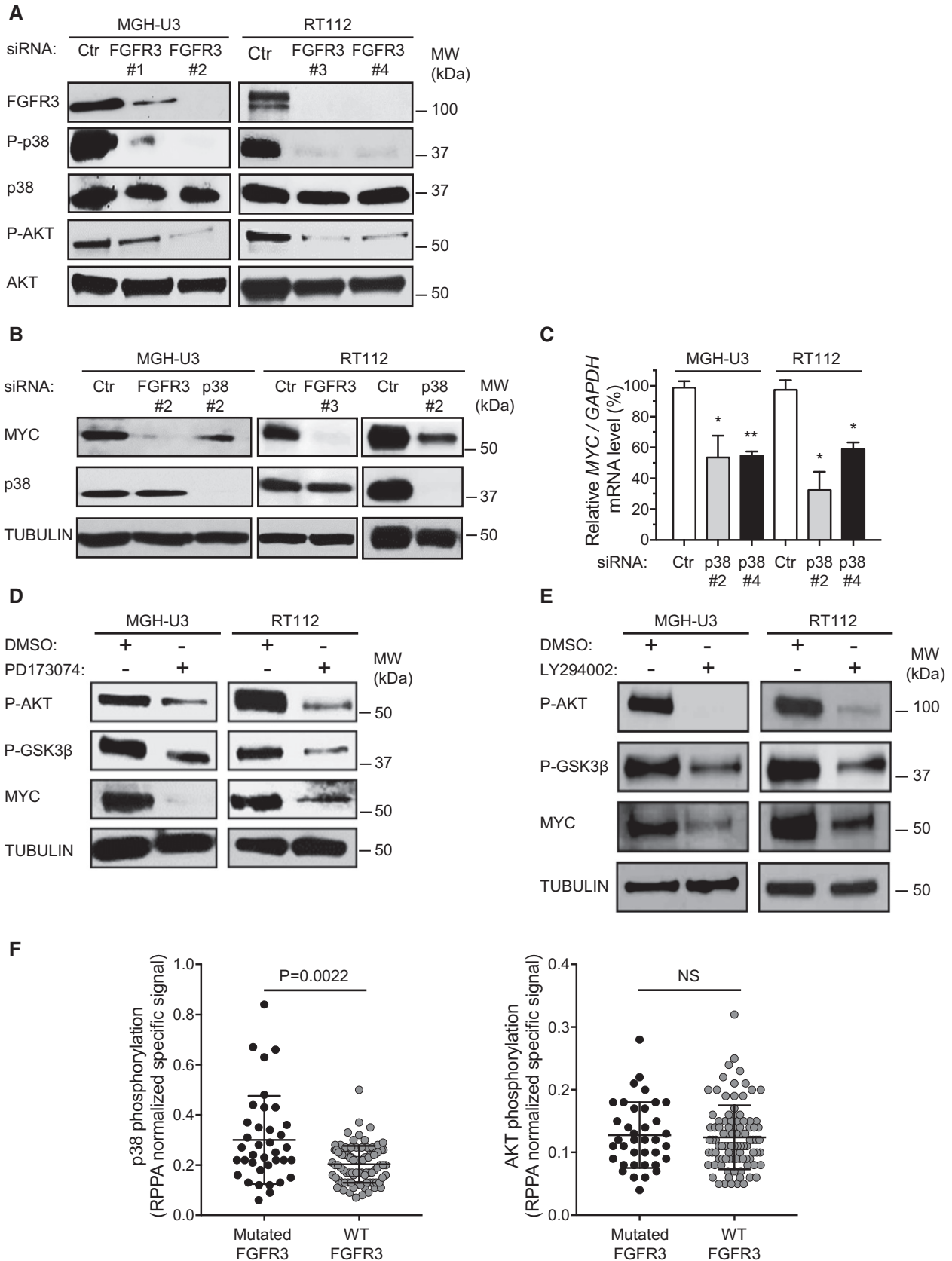


Figure 3.

Figure 3. The MYC accumulation induced by activated FGFR3 is dependent on the activation of p38 and AKT.

- A MGH-U3 and RT112 human bladder tumor cells were transfected with control siRNA (Ctr) or with siRNAs targeting *FGFR3*. Lysates were obtained and the levels of p38, phospho-p38 [P-p38 Thr180/Tyr182], AKT, phospho-AKT (P-AKT Ser473), and *FGFR3* were assessed by Western blotting. Different siRNAs were used in the two cell lines (see Materials and Methods).
- B MGH-U3 and RT112 cells were transfected for 72 h with a siRNA targeting either *FGFR3* or *MAPK14* (p38 α). Lysates were obtained and MYC and p38 protein levels were analyzed by Western blotting.
- C MGH-U3 and RT112 cells were transfected with *MAPK14* (p38 α) siRNA for 72 h. The level of MYC mRNA level was determined by RT-qPCR (left panel). The results presented are the means and standard errors of two independent experiments carried out in triplicate. Unpaired Student's *t*-tests were used for comparison with appropriate siRNA control (Ctr), **P* < 0.05; ***P* < 0.005.
- D MGH-U3 and RT112 cells were treated for 2 h with DMSO or a FGFR inhibitor (0.5 μ M PD173074). Lysates were obtained and analyzed by Western blotting with antibodies against MYC, phospho-AKT (Ser473) and phospho-GSK3 β (Ser9). Tubulin was used as a loading control.
- E Western blot comparing MYC, phospho-AKT (Ser473) and phospho-GSK3 β (Ser9) levels in MGH-U3 and RT112 cells treated for 3 h with a PI3 kinase inhibitor (20 μ M LY294002) or control DMSO. Tubulin was used as a loading control.
- F The level of phosphorylation of p38 (left panel) and AKT (right panel) was assessed by reverse-phase protein array (RPPA) in 129 human bladder tumors, as described in the Materials and Methods. *FGFR3* mutations were present in 38 tumors. No tumor harbored an *FGFR3*-TACC3 or *FGFR3*-BAIAP2L1 fusion gene. Mann-Whitney test was used for comparisons between mutated and non-mutated tumors. Means and standard errors are represented.

about 70% of NMIBCs and 20% of MIBCs. These alterations induce the constitutive activation of *FGFR3* and lead to an oncogene dependence to *FGFR3*. In this study, we characterized further the mechanisms involved in the activity of aberrantly activated *FGFR3*, highlighting new possibilities for the treatment of bladder tumors with activating alterations of *FGFR3*. We found that *MYC* played a crucial role in the aberrantly activated *FGFR3* pathway. This transcription factor regulated by *FGFR3* was involved in *FGFR3*-driven cell proliferation in two bladder cancer-derived cell lines expressing *FGFR3* (*FGFR3*-Y375C) or the fusion protein *FGFR3*-TACC3. We also showed that *MYC* upregulated *FGFR3* expression directly, by binding to enhancers upstream from *FGFR3*, as part of a *FGFR3*/*MYC* positive feedback loop operating both *in vitro* and *in vivo* in bladder cancer-derived cell lines xenografts and in a PDX model bearing an *FGFR3* mutation. The *FGFR3*-driven accumulation of *MYC* was due to both an increase in *MYC* mRNA levels and stabilization of the *MYC* protein. *FGFR3* increases *MYC* mRNA levels by activating the p38 α MAP kinase. *FGFR3* also induces stabilization of the *MYC* protein, by activating AKT, which, in turn, phosphorylates the Ser9 residue of GSK3 β , thereby preventing its interaction with *MYC* and the degradation of this protein by the proteasome. Finally, our results provide *in vitro* and *in vivo* proof of concept in xenografts that the inhibition of *MYC* expression, and, in turn, of *FGFR3* expression, by an inhibitor of AKT or p38 or a BET bromodomain inhibitor (JQ1) is a potentially effective strategy for the treatment of *FGFR3*-dependent bladder tumors. The results obtained with *FGFR3* inhibitors in one PDX model and in two cell lines xenografts were similar, increasing our confidence in the relevance of our results to human tumors. Based on the results presented here, we devised a model for this newly identified *FGFR3*/*MYC* positive feedback loop involved in bladder tumor cell proliferation (Graphical abstract). Interestingly, studies of *MYC* mRNA levels and of the phosphorylation of p38 and AKT in human bladder tumor samples harboring *FGFR3* mutations suggested that this loop might also operate in tumors. The relevance to human tumors was further supported by the decrease in *FGFR3* and *MYC* levels following anti-FGFR treatment in a PDX model bearing an *FGFR3* mutation. The insight into the aberrantly activated *FGFR3* pathway provided by this study could make it possible to identify tumors presenting alterations to this pathway, such as *MYC* overexpression or p38 activation, in the absence of *FGFR*-activating genetic alterations. These tumors might also benefit from the alternative therapeutic strategies

proposed in this study for bladder tumors displaying aberrant *FGFR3* activation.

We found that *FGFR3* activation increased *MYC* expression and that *FGFR3* was a direct transcriptional target of *MYC*. This *FGFR3*/*MYC* positive feedback loop probably contributes to the higher levels of *FGFR3* expression previously observed in human bladder tumors with *FGFR3* mutations (Bernard-Pierrot *et al*, 2006). It has been suggested that this overexpression is also mediated by a loss of microRNAs99/100 targeting *FGFR3* in bladder tumors (Catto *et al*, 2009; Blick *et al*, 2013).

In this study, we searched for transcriptional regulators involved in the regulation of gene expression induced by two types of aberrantly activated *FGFR3*: a mutated form of the receptor (Y375C) and a fusion protein (*FGFR3*-TACC3). Specific signaling pathways—PLC γ activation (Williams *et al*, 2013) and localization to the kinetochore (Singh *et al*, 2012)—have been associated with these two forms, but we observed a large overlap between the transcriptional regulators driven by these two types of receptors. Furthermore, both types of receptor acted via the same molecular mechanism, the activation of p38 and AKT, leading to *MYC* accumulation, resulting in the induction of hyperproliferation. Most of the upstream regulators activated by both types of receptor in this study have also been shown to be regulated by *FGFR3*-BAIAP2L1, another form of aberrantly activated *FGFR3*, in RAT2 cells (Nakanishi *et al*, 2015). In both this and a previous study, we found that *FGFR3* activation inhibited tumor suppressor pathways involving RB1/RBL1, TP53, or P16 (*CDKN2A*) and activated pro-proliferative pathways involving E2F, CCND1, or TBX2. However, the *MYC* activation described here was not observed in RAT2 cells. This discrepancy may reflect differences in the technical approach used (inhibition versus overexpression), the species and tissues studied (human epithelium versus rat fibroblast) or the thresholds used to identify genes regulated by *FGFR3*, and the upstream regulators involved in their regulation.

In a study using a very different approach published during the preparation of this manuscript, *MYC* was also implicated in pathways involving activated *FGFRs* in several different types of cancer (Liu *et al*, 2016). This study showed that the altered *FGFRs* were associated with an increase in *MYC* protein stability. In one cell line displaying *FGFR1* amplification, the authors showed, as suggested by our data for *FGFR3* revealing a lack of synergy between *MYC* and *FGFR3* knockdown, that *MYC* was the main effector of *FGFR1*

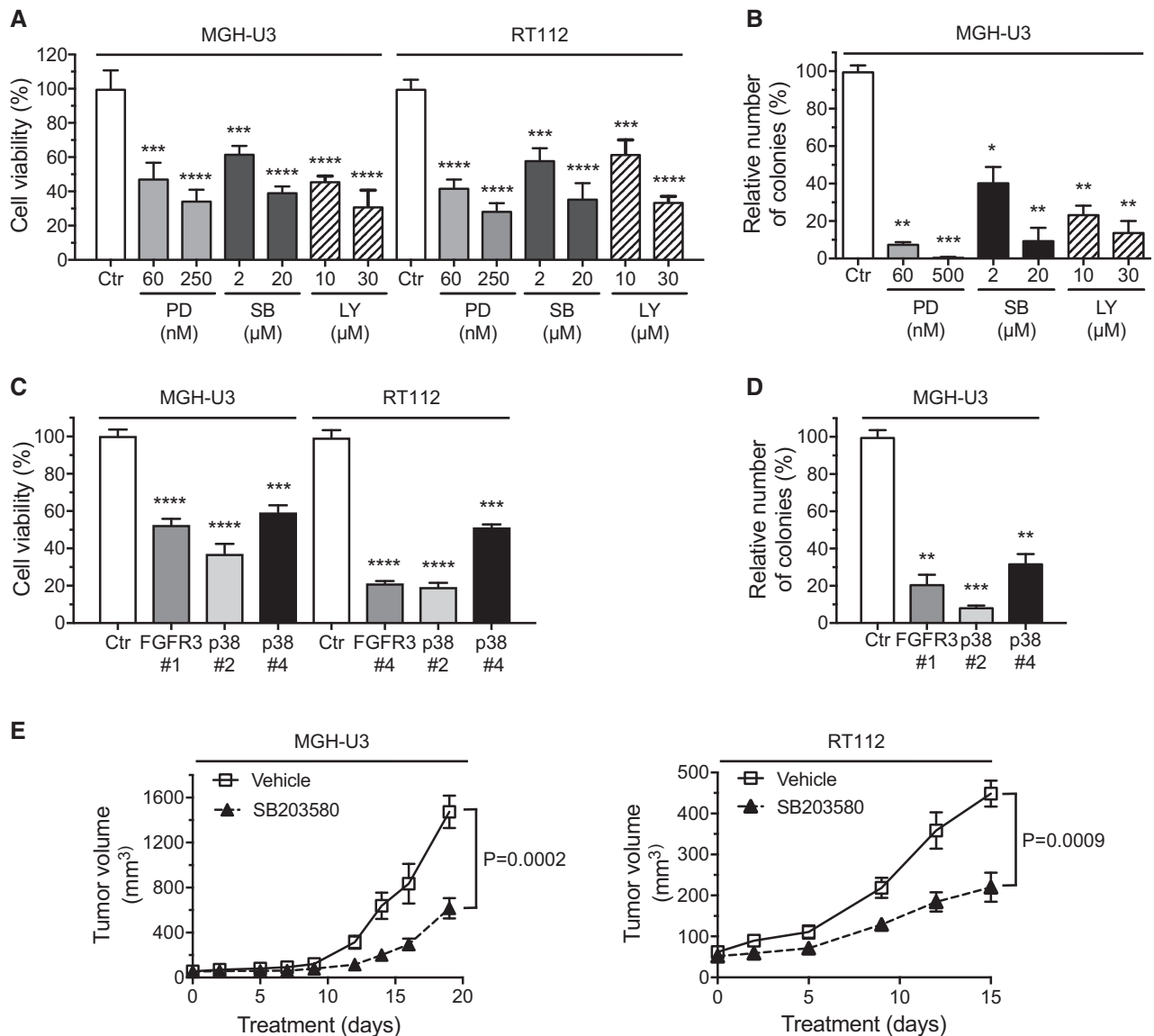


Figure 4. The inhibition of p38 or AKT reduces the growth and transformation of bladder cancer cells expressing aberrantly activated FGFR3.

A MGH-U3 and RT112 cells were treated with control DMSO, PD [PD173074 (FGFR inhibitor)], SB [SB203580 (p38 inhibitor)] or LY [LY294002 (PI3 kinase inhibitor)] for 72 h and cell viability was then assessed by measuring MTT incorporation.

B Impact of PD (PD173074), SB (SB203580), or LY (LY294002) treatment on the cell anchorage-independent growth of MGH-U3 cells. Colonies in soft agar with diameters greater than 50 μm were counted 14 days after seeding in the presence of inhibitors.

C Comparison of the effects of *MAPK14* (p38 α isoform) and *FGFR3* knockdown on the viability of MGH-U3 and RT112 cells, as measured by MTT incorporation.

D Soft agar colony formation assay for MGH-U3 cells transfected with siRNA against *FGFR3* or *MAPK14* (p38 α isoform). Cells were grown for 14 days before counting.

E MGH-U3 bladder cancer cells were injected into nude mice ($n = 5$ animals/group), two xenografts per animal (one in each flank). Nine days later, the mice received an injection of vehicle or SB203580 (100 μl of 20 μM SB203580) into the tumor, once daily, 6 days per week. Tumor size was measured at the indicated time point, and tumor volume was calculated.

Data information: (A–D) The results presented are the means of two independent experiments carried out in triplicate; the standard errors are indicated. Unpaired Student's *t*-tests were used to assess the significance of differences, * $P < 0.05$; ** $0.001 < P < 0.005$; *** $0.0001 < P < 0.001$; **** $P < 0.0001$. (E) Data are presented as means \pm SEM. Results were compared in Mann–Whitney test.

activity, because the effect of FGFR inhibitors was abolished by an undegradable MYC mutant. They suggested that MYC protein stabilization was due to the activation of ERK1/2, rather than AKT as described here. Our results clearly highlighted the crucial role of AKT in sustaining MYC stability through the phosphorylation of

GSK3 β . However, we did not study the impact of ERK1/2 inactivation in our FGFR3-dependent bladder tumor models and we cannot, therefore, rule out the possible involvement of this pathway in cooperation with the AKT pathway, as shown for RAS (Sears *et al*, 2000; Yeh *et al*, 2004). Furthermore, we also highlighted the role of

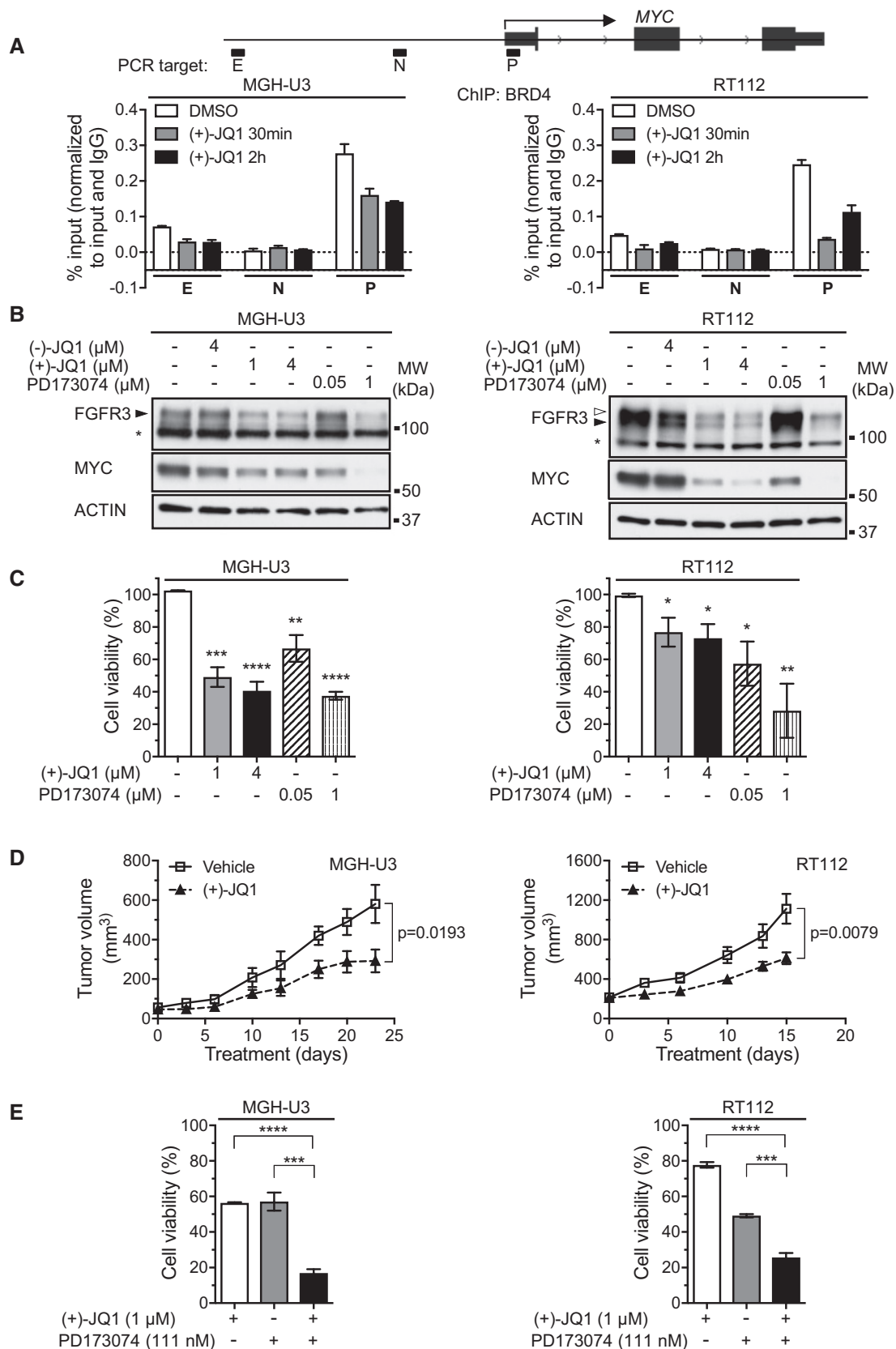


Figure 5.

Figure 5. The MYC accumulation induced by activated FGFR3 confers sensitivity to BET bromodomain inhibitors in FGFR3-dependent bladder cancer cells *in vitro* and *in vivo*.

- A The qPCR target loci for *MYC* are shown (upper panel). ChIP–qPCR of BRD4 for the *MYC* locus in MGH-U3 and RT112 cells treated with DMSO or 1 μ M (+)-JQ1 for 30 or 120 min (lower panels). Data presented are representative of two replicate experiments. Error bars show standard deviation of three replicate qPCR reactions.
- B Western blot analysis of *MYC* and *FGFR3* expression in lysates from MGH-U3 and RT112 cells treated with (+)-JQ1 (1 or 4 μ M) for 48 h. Anti-actin antibody was used as a loading control. Pan-FGFR inhibitor, PD173074 (50 nM and 1 μ M), and inactive enantiomer (–)-JQ1 (4 μ M) were used as controls. Black and white arrowheads indicate WT *FGFR3* and *FGFR3*-TACC3 bands, respectively. Asterisk indicates non-specific band.
- C MGH-U3 and RT112 cells were treated for 72 h with DMSO, (+)-JQ1 (1 or 4 μ M) or PD133074 (50 nM or 1 μ M). Cell viability was measured with CellTiter-Glo. Results were compared with those for a DMSO control in unpaired Student's *t*-tests, * P < 0.05; **0.001 < P < 0.005; ***0.0001 < P < 0.001; **** P < 0.0001. Means and standard errors are represented. Three replicates were performed.
- D MGH-U3 and RT112 bladder cancer cells were injected into nude mice (n = 6 animals/group), two xenografts per animal (one in each flank). Nine and seven days later, the mice received an injection of vehicle or (+)-JQ1 (IP injection, 50 mg/kg, once daily, 6 days per week), respectively. Tumor growth was assessed twice weekly, by measuring tumor size. Data are presented as means \pm SEM. Results were compared in Wilcoxon's test.
- E MGH-U3 and RT112 cells were treated for 72 h with (+)-JQ1 and PD133074 alone or in combination. Cell viability was measured with CellTiter-Glo. Data are presented as means \pm SD of three experiments carried out in triplicate. Results for the drug combination were compared with those for each individual drug separately, in unpaired Student's *t*-tests, ***0.0001 < P < 0.001; **** P < 0.0001.

Source data are available online for this figure.

mutated *FGFR3*, dependent on p38 activation, in the upregulation of *MYC* mRNA levels both in cell lines and in a PDX model. *MYC* overexpression which often leads to *MYC* oncogene addiction has been associated with aggressive phenotype in many tumor types (Dang, 2012; Stine *et al*, 2015). This is not the case in bladder cancer since the majority of *FGFR3*-mutated tumors are low-stage, low-grade tumors. Furthermore, among *FGFR3*-mutated tumors, no difference in *MYC* expression could be observed in MIBC and NMIBC (data not shown). This could be related to a specific *FGFR3*-induced *MYC* transcriptomic program in bladder tumors (Kress *et al*, 2015). Consistent with its key role in *FGFR* signaling, *MYC* was also recently identified as a potential marker of the anti-*FGFR* response, because cells expressing both *MYC* and *FGFRs* have been shown to be more sensitive to anti-*FGFR* therapies (Malchers *et al*, 2014; Liu *et al*, 2016). In light of its key role downstream from *FGFR*, *MYC* inhibition appears to be a valuable therapeutic strategy for bladder tumors with *FGFR3* alterations. *MYC* has emerged as a clear therapeutic target in other cancers, and many strategies for inhibiting *MYC* activity through direct or indirect means have been described (Posternak & Cole, 2016). We evaluated the therapeutic potential of BET bromodomain inhibitors, a class of epigenetic modulators that emerged in a clinical setting. We demonstrated that JQ1 prevented BRD4 binding to the *MYC* promoter and enhancer, thereby inhibiting *MYC* expression and, consequently, the growth of bladder tumor cells expressing activated forms of *FGFR3* both *in vitro* and *in vivo* in xenograft. These preclinical results suggest that bladder tumors with *FGFR3* alterations could potentially be treated with BET bromodomain inhibitors. Resistance to monotherapy with BET bromodomain inhibitors has been observed and linked to kinome reprogramming in ovarian cancer (Kurimchak Alison *et al*, 2016) or to a decrease in PP2A activity in triple-negative breast cancer (Shu *et al*, 2016). Resistance to anti-*FGFR* therapies has also been observed in *FGFR3*-dependent cells and linked to the activation of ERBB2/3 or EGFR (Herrera-Abreu *et al*, 2013; Wang *et al*, 2015). These observed resistances could be overcome by combination strategies, involving PI3K inhibitors, for example (Wang *et al*, 2017). The use of a combination of a pan-*FGFR* inhibitor and a BET bromodomain inhibitor induced a stronger growth inhibition as compared to each individual drug *in vitro*. *In vivo* tests for these treatments are currently underway for our PDX model.

We also demonstrated that the activation of both p38 and AKT was critical for the induction of bladder cancer cell proliferation and transformation by *FGFR3*. This critical role was linked to the ability of these two pathways to induce *MYC* accumulation, by increasing *MYC* mRNA levels and by stabilizing the *MYC* protein, respectively. The role of AKT in cancer progression has been clearly demonstrated for various tumors (Vivanco & Sawyers, 2002), including bladder cancer (Calderaro *et al*, 2014). The role of p38 in cancer is dual, p38 playing both a tumor suppressor role by inducing cell apoptosis and protumorigenic functions depending on the cancer types (Koul *et al*, 2013; Igea & Nebreda, 2015). The opposite functions could be related to cell specificity, nature of the stimuli, the isoform activated since p38 exist as four isoforms or the component downstream p38. p38 can be activated by tyrosine kinase receptors (PDGF receptor, VEGF receptor, EGF receptor, *FGFR1*) to function as a positive regulator of tumor progression, mediating motility and invasion, suppressing apoptosis, stimulating the epithelial-to-mesenchymal transition in various cell types (Bates & Mercurio, 2003; Frey *et al*, 2004; Nishihara *et al*, 2004). Our results demonstrating that p38 α promotes proliferation, by upregulating *MYC* mRNA levels are in line with the protumorigenic functions of p38 and with recent studies in breast, head and neck cancers and nasopharyngeal carcinoma (Leelahavanichkul *et al*, 2014; Li *et al*, 2017; Wada *et al*, 2017). The activation of p38 by activated-*FGFR3* in bladder tumors contributes to malignant behavior and the inhibition of this activation may be of therapeutic value, as reported for an increasing number of cancers (Koul *et al*, 2013; Igea & Nebreda, 2015).

Our results thus suggest alternative strategies targeting different aspects of *FGFR3* signaling that might be beneficial for the treatment of bladder tumors expressing aberrantly activated *FGFR3*. Targeting two parts of the signaling pathway simultaneously may increase treatment efficacy or delay the development of tumor resistance, as observed clinically in melanomas harboring *RAF* mutations managed with treatments targeting *RAF* and *MEK* (Flaherty *et al*, 2012). It has already been reported that of the simultaneous inhibition of *FGFR3* and *AKT* in MGH-U3 xenograft models increases treatment efficacy over than achieved with either of the two drugs used separately (Davies *et al*, 2015). Such strategies are widely tested in different tumor types and in

particular using pan-FGFR inhibitors. A multi-drug phase II clinical trial including pan-FGFR inhibitor (BGJ398) together with a MEK inhibitor (MEK162) and a RAF inhibitor (LGX818) is currently ongoing in advanced BRAF melanoma (NCT02159066). A phase Ib trial of BGJ398 in combination with BYL719 (PI3K inhibitor) on solid tumors showed encouraging results as eight patients over 24 showed a partial response, among them, one patient with a urothelial carcinoma bearing FGFR3-TACC3 had a complete tumor shrinkage for 4 months (NCT01928459). FGFR3-TACC3 fusion protein expression has been reported in several other cancers, including glioblastoma (Singh *et al*, 2012) and lung adenocarcinoma (Capelletti *et al*, 2014). It would be interesting to determine whether this FGFR3/MYC feedback loop, mediated by AKT and p38, also operates in other types of human cancers expressing FGFR3-TACC3. If so, these treatments could be extended to other cancer types.

Materials and Methods

Cell culture and transfection

The human bladder-derived cell lines RT112, RT4, UM-UC-14, and UM-UC-5 were obtained from DSMZ (Heidelberg, Germany). MGH-U3 cells were kindly provided by Dr. Paco Real (CNIO, Madrid). We mostly used RT112 and MGH-U3 cells. RT112 cells were derived from a transitional cell carcinoma (TCC; histological grade G2) excised from a woman with untreated primary urinary bladder carcinoma. The MGH-U3 cell line was established with cells from a 76-year-old patient with a history of recurrent non-invasive bladder carcinomas (papillary TCC, histological grade G1; Lin *et al*, 1985). MGH-U3 cells harbor a homozygous FGFR3-Y375C mutation and RT112 cells have a FGFR3-TACC3 translocation. A comprehensive genomic characterization of these cells has been reported (Earl *et al*, 2015). MGH-U3, UM-UC-5, and UM-UC-14 cells were cultured in DMEM, whereas RT112 and RT4 cells were cultured in RPMI. Media were supplemented with 10% fetal calf serum (FCS). Cells were incubated at 37°C, under an atmosphere containing 5% CO₂. The identity of the cell lines used was checked by analyzing genomic alterations with comparative genomic hybridization arrays (CGH array), and the *FGFR3* and *TP53* mutations were checked with the SNaPshot technique (for *FGFR3*) or by classical sequencing (for *TP53*), the results obtained being compared with the initial description of the cells. We routinely checked for mycoplasma contamination.

Transfected NIH-3T3 cells expressing the mutated human FGFR3b-S249C receptor (clones S249C1.1, S249C 1.2) or transfected with the control pcDNA1-Neo plasmid (clones Neo1.5, Neo 2.1) were established during a previous study (Bernard-Pierrot *et al*, 2006). They were cultured in DMEM supplemented with 10% newborn calf serum (NCS), 2 mM glutamine, 100 U/ml penicillin, 100 µg/ml streptomycin, and 400 µg/ml G418.

For siRNA transfection, MGH-U3 and RT112 cells were used to seed six-well or 24-well plates at a density of 250,000 cells/well for MGH-U3 cells and 200,000 cells/well for RT112 cells. Cells were transfected with 5 (*FGFR3* siRNA #3 and #4) or 20 nM siRNA in the presence of Lipofectamine RNAi Max reagent (Invitrogen), in accordance with the manufacturer's protocol. siRNAs were purchased

from Ambion and Qiagen. For the control siRNA, we used a Qiagen control targeting luciferase (SI03650353).

The sequences of the siRNAs were as follows:

FGFR3 #1	5'-GCUUUACCUUUUAUGCAA-3' (sense strand)
	5'-UUGCAUAAAAGGUAAGGC-3' (antisense strand)
FGFR3 #2	5'-GGGAAGCCGUGAAUUCAGU-3' (sense strand)
	5'-ACUGAAUUCACGGUCC-3' (antisense strand)
FGFR3 #3	5'-CCGUAGCCGUGAAGAUC-3' (sense strand)
	5'-AGCAUCUUCACGGCUACGG-3' (antisense strand)
FGFR3 #4	5'-CCUGCGUCGUGGAGAACA-3' (sense strand)
	5'-UUGUUCUCCACGACGAG-3' (antisense strand)

FGFR3 siRNA#1 and siRNA#2 targeted exon 19 of *FGFR3* (NM_001163213). They therefore knocked down the expression of wild-type and mutated *FGFR3*, but not of the *FGFR3*-fusion gene containing the first 18 exons of *FGFR3* (Wu *et al*, 2013). Conversely, siRNA#3 and siRNA#4 targeted exons 12 and 6 of *FGFR3* (NM_001163213), respectively, knocking down both wild-type and *FGFR3*-TACC3 expression in RT112 cells.

p38α #2	5'-GGUCUCUGGAGAAUCAA-3' (sense strand)
	5'-UUGAAUUCUCCGAGACC-3' (antisense strand)
p38α #4	5'-CUGCGGUUACUAAACAUA-3' (sense strand)
	5'-UAUGUUUAAAGUAACCGCAG-3' (antisense strand)
p38α refers to <i>MAPK14</i>	
MYC #1	5'-UCCCGGAGUUGGAAACAATT-3' (sense strand)
	5'-UUGUUUCCAUCUCCGGGATC-3' (antisense strand)
MYC #2	5'-CGGUGCAGCCGUUUUCUATT-3' (sense strand)
	5'-UAGAAUACGGCUGCACCGAG-3' (antisense strand)

Cell viability was assessed with the MTT assay (0.5 mg/ml) in 24-well plates, or the CellTiter-Glo assay (Promega) in 96-well plates, 72 h after transfection. Cell lysates were also prepared 72 h after transfection, in six-well plates, for subsequent immunoblotting analysis.

Kinase and protein inhibitors

The inhibitors LY294002, PD98059, SB203580, SU5402, and PD173074 were purchased from Calbiochem (Merck Eurolab, Fontenay Sous Bois, France). MG132 was obtained from Selleckchem (Euromedex, Souffelweyersheim, France). BGJ398 was purchased from LC Laboratories (USA).

The inhibitors (+)-JQ1, (−)-JQ1 and PD173074 (for *in vivo* studies) were purchased from MedChem Express (MedChemtronica, Stockholm, Sweden).

Immunoblotting

NIH-3T3, MGH-U3, RT112, RT4, UM-UC-14, and UM-UC-5 cells were resuspended in Laemmli lysis buffer [50 mM Tris-HCl (pH 6.8), 2 mM DTT, 2.5 mM EDTA, 2.5 mM EGTA, 2% SDS, 5% glycerol with protease inhibitors and phosphatase inhibitors

(Roche)], and the resulting lysates were clarified by centrifugation. The protein concentration of the supernatants was determined with the BCA protein assay (Thermo Scientific, France). Proteins (10–50 µg) were resolved by SDS–PAGE in 10% polyacrylamide gels, electrotransferred onto Bio-Rad nitrocellulose membranes, and analyzed with antibodies against p38 and the phosphorylated form of p38 (Thr180/Tyr182; Cell Signaling Technology # 9212 and # 4511, used at 1/5,000), AKT and the phosphorylated form of AKT (Ser473; Cell Signaling Technologies # 2920 and # 4060, used at 1/5,000), GSK3β (Ser9; Cell Signaling Technology # 5558, used at 1/1,000), MYC (Cell Signaling Technology # 9402, used at 1/1,000), α-tubulin and β-actin (Sigma Aldrich #T6199, used at 1/15,000 and #A2228, used at 1/25,000), or the extracellular domain of FGFR3 (Abcam, # ab133644, 1/5,000). Anti-mouse IgG, HRP-linked, and anti-rabbit IgG, HRP-linked antibody (Cell Signaling Technology # 7076 and # 7074, used at 1/3,000) were used as secondary antibodies. Protein loading was checked by Amido Black staining of the membrane after electrotransfer.

ChIP–qPCR

RT112 and MGH-U3 cells were cross-linked directly by adding 1% formaldehyde to the medium and incubating for 10 min at room temperature. The reaction was stopped by adding glycine to a final concentration of 0.125 M and incubating for 5 min at room temperature. The cells were then harvested. The fixed cells were rinsed twice with PBS, resuspended in extraction buffer [0.25 M sucrose, 10 mM Tris–HCl pH 8, 10 mM MgCl₂, 1% Triton, 5 mM β–mercaptoethanol, protease inhibitors (Roche)] and centrifuged at 3,000 × g for 10 min. We then used the ChIP–IT[®] High Sensitivity kit (Active motif), treating the samples according to the manufacturer's instructions. ChIP was performed with the following antibodies: mouse anti-BRD4 (Bethyl Laboratories A301-985A50), rabbit polyclonal anti-c-MYC (Santa Cruz sc-764), anti-H3K4me3 (Abcam ab8580-25), and anti-H3K27ac (Abcam ab4729) antibodies and the rabbit IgG polyclonal isotype control antibody (Abcam ab37415).

For ChIP–qPCR experiments, quantitative PCR was performed with the SYBR Green PCR kit from Applied Biosystems. Enrichment in ChIPed DNA was calculated as a percentage of the input minus IgG ChIP signal. The sequences of the primers used were as follows:

FGFR3 locus		
E1	AAGATGAGCAAGGCACCTG (forward)	CTCCAGGTCAGAACCAAAGC (reverse)
E2	ACACGCAGGCACACACAG (forward)	AGGGCTTGTGCTCCTCTG (reverse)
P	GCAGGTAAGAAGGGACCCAC (forward)	CGGAATCCGGGCTCTAACC (reverse)
N	ACTCCTTCGACACCTGCAAG (forward)	GTCCTGAAGGTGAGCTGCT (reverse)
MYC locus		
E	TCTTGCCAGACCTAATGCTG (forward)	CCTTGCCACATTGCTTATC (reverse)
N	CAGCTAAATGGCACATAGGC (forward)	ATATTGCCCGGCTAATCTC (reverse)
P	TTCGGGTAGTGGAAAACCAG (forward)	GTGCAATAGCGCAGGAATG (reverse)

Soft agar assay

MGH-U3 cells (20,000), untransfected or transfected with siRNA, were used to seed 12-well plates containing DMEM supplemented with 10% FCS and 1% agar, in triplicate. Cells were cultured in the presence or absence of inhibitors in the agar and culture medium, as appropriate. The medium was changed weekly. The plates were incubated for 14 days, and colonies larger than 50 µm in diameter, as measured with a phase-contrast microscope equipped with a measuring grid, were counted.

RNA extraction from cell lines

RNA was isolated from cell lines with RNeasy Mini kits (Qiagen, Courtaboeuf, France).

Real-time reverse transcription-quantitative PCR

Reverse transcription was performed with 1 µg of total RNA, with the High-Capacity cDNA reverse transcription kit (Applied Biosystems), and MYC and GAPDH and TATA-box binding Protein (TBP) were amplified by PCR in a Roche real-time thermal cycler, with the Roche Taqman master mix (Roche) with the Hs00153408_m1, Hs02758991_g1 and 4326322E assays on demand (encompassing primers and Taqman probes) purchased from Applied Life Technologies.

DNA array

For the identification of genes displaying changes in expression after the depletion of FGFR3 in MGH-U3 cells, we transfected the cells for 72 h with FGFR3 siRNA#1, FGFR3 siRNA#2 or SMARTpool: ON-TARGETplus FGFR3 siRNA (Dharmacon, L-0031333-00-0005). For the identification of genes displaying a change in expression after FGFR3 depletion in RT112 cells, we transfected the cells for 40 h with FGFR3 siRNA#3 or FGFR3 siRNA#4. mRNA was extracted and purified with RNeasy Mini kits (Qiagen). Total RNA (200 ng) from control and siRNA-treated MGH-U3 and RT112 cells was analyzed with the Affymetrix human exon 1.0 ST DNA array and the Affymetrix U133 plus 2 DNA array, respectively, as previously described for PPARG-regulated genes (Biton et al, 2014). The microarray data described here are available from GEO (<https://www.ncbi.nlm.nih.gov/geo/>) under accession number GSE84733. The LIMMA algorithm was used to identify genes differentially expressed between FGFR3 siRNA-treated (two and three different siRNAs were used for RT112 and MGH-U3 cells, respectively) and Lipofectamine-treated cells (three replicates; Ritchie et al, 2015). The P-values were adjusted for multiple testing by Benjamini–Hochberg FDR methods. Genes with a log₂ fold-change of at least 0.58, in a positive or negative direction, with a FDR below 5%, were considered to be differentially expressed.

Human bladder samples

We used protein extracted from 129 human bladder tumors (57 non-muscle-invasive and 72 muscle-invasive tumors) for RPPA analysis (Calderaro et al, 2014). The flash-frozen tumor samples were stored at –80°C immediately after transurethral resection or

cystectomy. All tumor samples contained more than 80% tumor cells, as assessed by the hematoxylin and eosin (H&E) staining of histological sections adjacent to the samples used for transcriptome analyses. All subjects provided informed consent, and the study was approved by the institutional review boards of the Henri Mondor, Foch and Institut Gustave Roussy Hospitals. RNA, DNA, and protein were extracted from the surgical samples by cesium chloride density centrifugation, as previously described (Calderaro *et al*, 2014). *FGFR3* mutations were studied with the SNaPshot technique. The expression of *FGFR3-TACC3* and *FGFR3-BAIAP2L1* was analyzed by PCR, as previously described (Wu *et al*, 2013).

Lyophilized proteins were solubilized in Laemmli sample buffer and boiled for 10 min. Protein concentrations were determined with the Bio-Rad Bradford Protein Assay Kit (Bio-Rad, France).

Reverse-phase protein array (RPPA)

Reverse-phase protein array with specific anti-phospho-AKT (S473; Cell Signaling Technology # 4058, used at 1/1,000) and anti-phospho-p38 (T180/Y182; BD Biosciences #612288, used at 1/500) antibodies was performed and analyzed as previously described (Calderaro *et al*, 2014). The specificity of the antibodies used for RPPA for the protein of interest was checked by Western blotting with 18 tumor lysates, before the study. We obtained a Pearson coefficient for the correlation between RPPA and Western blotting of 0.84 for P-AKT (66) and 0.88 for P-p38 (data not shown).

In vivo models

Mouse experiments reported herein were approved by Animal Housing and Experiment Board of the French government.

Xenograft models

Six-week-old female Swiss *nu/nu* mice (Charles River Laboratories) were raised in the animal facilities of Institut Curie, in specific pathogen-free conditions. They were housed and cared for in accordance with the institutional guidelines of the French National Ethics Committee (*Ministère de l'Agriculture et de la Forêt, Direction de la Santé et de la Protection Animale*, Paris, France), under the supervision of authorized investigators. Mice received a subcutaneous injection, into each flank (dorsal region), of 5×10^6 RT112 or MGH-U3 bladder cancer cells in 100 μ l PBS. For each study, with each of the cell lines, mice were randomly separated into two groups when tumors reached a volume of 100 mm³ (± 20). For *FGFR3* inhibition studies, the mice were treated daily for 9 days, by oral gavage with PD173074 (25 mg/kg; $n = 4$) in one group and with vehicle (0.05 M acetate buffer) in the other ($n = 4$). The tumors were then removed. Part of the tumor was flash-frozen in liquid nitrogen for protein extraction in Laemmli buffer. For p38 inhibition studies, one group received daily injections of SB203580 (100 μ l, 20 μ M) into the tumor ($n = 5$), whereas the other group received daily injections of vehicle (PBS; $n = 5$). For JQ1 treatment, mice received a daily intraperitoneal injection of 50 mg/kg JQ1 ($n = 6$) or vehicle (10% DMSO, 90% 10% 2-hydroxypropyl β -cyclodextrin; $n = 6$). For each treatment, the tumor was measured twice weekly with calipers, and its volume in mm³ was calculated with the formula: $\pi/6 \times (\text{largest diameter}) \times (\text{shortest diameter})^2$.

Patient-derived Tumor Xenograft (PDX) model (F659)

A patient-derived bladder cancer xenograft model (F659) was established as follow. A fresh specimen was collected from a patient diagnosed with a muscle-invasive bladder carcinoma with two positive perivesical lymph nodes (pT3bN2Mx), in accordance with French regulations concerning patient information and consent and then xenografted subcutaneously in the interscapular space of 5-week-old male Swiss *nu/nu* mice (Charles River Laboratories) and serially passaged into male Swiss *nu/nu* mice (Charles River Laboratories). DNA was isolated from snap-frozen tumor from the patient and from the PDX tumor (at passage 3 in mice), with a classical phenol-chloroform-isoamyl alcohol extraction protocol. *FGFR3* mutations were studied by the SNaPshot method, as previously described (van Oers *et al*, 2005), and a *FGFR3-S249C* heterozygous mutation was detected in both samples.

For treatment with the pan-FGFR inhibitor, BGJ398, PDX (F659) tumor tissue at passage 4 in mice was cut into small pieces (5 mm³) and subcutaneously xenografted into multiple mice in the interscapular region. When tumor sizes reached 100–200 mm³, mice were randomly divided into two groups and treated by daily oral gavage with BGJ398 (30 mg/kg, LC Laboratories) or vehicle (0.05 M acetate buffer). Tumor growth was measured twice weekly with an electronic caliper, and tumor volume was calculated and expressed relative to the initial size of the tumor. Two experiments were conducted as follows: one for a long-term treatment (29 days; $n = 5$ animal per group) in which tumors were monitored for two additional weeks after the end of treatment, and one for a short-term treatment over a period of 4 days ($n = 4$ animal per group). The mice were sacrificed at the end of the experiments. Their tumors were harvested and flash-frozen. RNA was isolated with Trizol, and proteins were recovered by lysis in Laemmli buffer for subsequent RT-qPCR and Western blot analyses, respectively.

Statistical analysis

Linear models for microarray data (LIMMA) was used to analyze DNA array experiments involving simultaneous comparisons between large numbers of RNA targets (Ritchie *et al*, 2015). All functional experiments were carried out twice or three times, in triplicate. Data are expressed as means \pm SD. Tukey's tests were used for multiple comparisons, and unpaired Student's *t*-tests (two-tailed) or Mann-Whitney *U*-tests were used for other statistical analyses. The control siRNA group, the IgG group, or the vehicle group was used as the reference group, depending on the experiment. The RPPA signals of tumors with and without *FGFR3* mutations were compared in Wilcoxon's rank sum tests. Non-parametric Spearman's rank correlation tests were carried out to evaluate the correlation between levels of *MYC* and *FGFR3* mRNA in human bladder tumors.

Data availability

Transcriptomic data obtained with Affymetrix U133plus2.0 DNA arrays for our CIT-cohorts of bladder tumors, encompassing 82 NMIBCs and 85 MIBCs, were previously deposited on the publicly available ArrayExpress databases E-MTAB-1803 and E-MTAB-1940, respectively (El Behi *et al*, 2013; Biton *et al*, 2014; Rebouissou *et al*, 2014). RNA-Seq data for an independent cohort of 416 tumors were available from ArrayExpress E-MTAB-4321 (Hedegaard *et al*, 2016).

The paper explained

Problem

Bladder cancer is the ninth most common cancer worldwide. FGFR3 alterations (mutations or translocations) are among the most frequent genetic events in bladder carcinoma. They lead to constitutive activation of the receptor and to oncogene addiction to FGFR3. Anti-FGFR therapies have recently yielded promising results, but the efficacy of such targeted therapies is currently limited by the emergence of resistance. In this study, we investigated the molecular mechanisms underlying the oncogenic activity of activated FGFR3 in bladder tumors, with a view to identifying new drug targets to improve treatment efficacy and/or limit resistance.

Results

We identified MYC as a key master regulator of proliferation activated by aberrantly activated FGFR3 in bladder cancer-derived cell lines. We showed that *FGFR3* is a direct target gene of MYC establishing an FGFR3/MYC positive feedback loop. Consistently, we found that human bladder tumors bearing *FGFR3* mutations had levels of *FGFR3* and *MYC* expression that were positively correlated. Further evidence of relevance to human tumors was provided by the use of a PDX model carrying an *FGFR3* mutation, in which FGFR3 inhibition induced a decrease in the expression of both MYC and FGFR3. We demonstrated that this loop was dependent on the activation of p38 and AKT by FGFR3, regulating *MYC* mRNA levels and protein stability, respectively. We showed that p38 and AKT activity were required for FGFR3-induced cell proliferation. Finally, we demonstrated that JQ1, a BET bromodomain inhibitor, was able to prevent *MYC* and *FGFR3* expression. JQ1 treatment significantly decreased cell viability *in vitro* and tumor outgrowth in a xenograft model.

Impact

We have identified a novel FGFR3-MYC positive feedback loop in bladder tumor cell lines harboring aberrantly activated FGFR3, which may be of clinical relevance, because it was also found in a PDX model harboring an *FGFR3* mutation. We also provide the first proof of concept that disrupting this loop with various inhibitors of FGFR3, p38, or AKT or with BET bromodomain inhibitors (JQ1) is of potential therapeutic value. These findings open up new possibilities for the treatment of bladder tumors displaying aberrant FGFR3 activation. The simultaneous inhibition of two targets from the same pathway may increase efficacy and prevent the development of resistance, as reported for the use of BRAF and MEK inhibitors for the treatment of melanoma with *BRAF* mutations.

FGFR3 mutational status and data for eight normal samples were kindly provided by Dr. Ellen Zwarthoff (Erasmus MC Cancer Institute, the Netherlands) and Dr. Lars Dyrskjøl (Aarhus University Hospital, Denmark). The microarray for MGH-U3 and RT112 cells treated with *FGFR3* siRNA are available from GEO (<https://www.ncbi.nlm.nih.gov/geo/>) under accession number GSE84733.

Expanded View for this article is available online.

Acknowledgements

We thank David Gentien and Leanne De Koning from the genomics and RPPA platforms, respectively, of Institut Curie. We thank Ellen Zwarthoff (Erasmus MC Cancer Institute, the Netherlands) and Dr. Lars Dyrskjøl (Aarhus University Hospital, Denmark) for providing *FGFR3* mutations for their cohort of tumors for which transcriptomic data were publicly available and transcriptomic data for eight normal samples, respectively. This work was supported by a grant from *Ligue Nationale Contre le Cancer* (IBP, FR, MM, HNK, RN, CK, MDG) as an

associated team (*Equipe labellisée*), the “*Carte d'Identité des Tumeurs*” program initiated, developed, and funded by *Ligue Nationale Contre le Cancer*, the “LIONS” project funded by INSERM/ITMO Cancer and the “Tumult” project funded by INCa. HNK and VSQ were supported by a fellowship from *Ligue Nationale Contre le Cancer*.

Author contributions

MM, FD, HN-K, CP, FR, and IB-P designed the study. MM, FD, HN-K, AM-V, CB, MS, IH VS-Q, CK, MD-G, and IB-P performed experiments and analyzed data. FD, EC, and RN carried out bioinformatics analyses. CB, HL, and TM established the PDX model. IB-P supervised the study. MM, FD, HN-K, FR, and IB-P wrote the manuscript. All authors made comments on the manuscript.

Conflict of interest

The authors declare that they have no conflict of interest.

References

- Abbosh PH, McConkey DJ, Plimack ER (2015) Targeting signaling transduction pathways in bladder cancer. *Curr Oncol Rep* 17: 58
- Antoni S, Ferlay J, Soerjomataram I, Znaor A, Jemal A, Bray F (2017) Bladder cancer incidence and mortality: a global overview and recent trends. *Eur Urol* 71: 96–108
- Bajorin D, Plimack ER, Seifker-radtke A, Choueiri TK, Wit RD, Sonpavde G, Gipson A, Brown H, Mai Y, Pang L *et al* (2015) Keynote-052: Phase 2 study of pembrolizumab (MK-3475) as first-line therapy for patients with unresectable or metastatic urothelial cancer ineligible for cisplatin-based therapy. *J Clin Oncol* 33: 3475
- Barfeld SJ, Urbanucci A, Itkonen HM, Fazli L, Hicks JL, Thiede B, Rennie PS, Yegnasubramanian S, DeMarzo AM, Mills IG (2017) c-Myc antagonises the transcriptional activity of the androgen receptor in prostate cancer affecting key gene networks. *EBioMedicine* 18: 83–93
- Bates RC, Mercurio AM (2003) Tumor necrosis factor- α stimulates the epithelial-to-mesenchymal transition of human colonic organoids. *Mol Biol Cell* 14: 1790–1800
- Bellmunt J, de Wit R, Vaughn DJ, Fradet Y, Lee JL, Fong L, Vogelzang NJ, Climent MA, Petrylak DP, Choueiri TK *et al* (2017a) Pembrolizumab as second-line therapy for advanced urothelial carcinoma. *N Engl J Med* 376: 1015–1026
- Bellmunt J, Powles T, Vogelzang NJ (2017b) A review on the evolution of PD-1/PD-L1 immunotherapy for bladder cancer: the future is now. *Cancer Treat Rev* 54: 58–67
- Bernard-Pierrot I, Brams A, Dunois-Lardé C, Caillaud A, Diez de Medina SG, Cappellen D, Graff G, Thiery JP, Chopin D, Ricol D *et al* (2006) Oncogenic properties of the mutated forms of fibroblast growth factor receptor 3b. *Carcinogenesis* 27: 740–747
- Billerey C, Chopin D, Bralet M-P, Lahaye J-B, Abbou CC, Bonaventure J, Zafrani S, Kwast TVD, Thiery JP, Radvanyi F (2001) Frequent *FGFR3* mutations in papillary non-invasive bladder (pTa) tumors. *Am J Pathol* 158: 1955–1959
- Biton A, Bernard-Pierrot I, Lou Y, Krucker C, Chapeaublanc E, Rubio-Pérez C, López-Bigas N, Kamoun A, Neuzillet Y, Gestraud P *et al* (2014) Independent component analysis uncovers the landscape of the bladder tumor transcriptome and reveals insights into luminal and basal subtypes. *Cell Rep* 9: 1235–1245
- Blick C, Ramachandran A, Wigfield S, McCormick R, Jubb A, Buffa FM, Turley H, Knowles MA, Cranston D, Catto J *et al* (2013) Hypoxia regulates *FGFR3*

- expression via HIF-1 α and miR-100 and contributes to cell survival in non-muscle invasive bladder cancer. *Br J Cancer* 109: 50–59
- Calderaro J, Rebouissou S, de Koning L, Masmoudi A, Héroult A, Dubois T, Maille P, Soyeux P, Sibony M, de la Taille A et al (2014) PI3K/AKT pathway activation in bladder carcinogenesis. *Int J Cancer* 134: 1776–1784
- Capelletti M, Dodge ME, Ercan D, Hammerman PS, Park SI, Kim J, Sasaki H, Jablons DM, Lipson D, Young L et al (2014) Identification of recurrent FGFR3-TACC3 fusion oncogenes from lung adenocarcinoma. *Clin Cancer Res* 20: 6551–6558
- Catto JWF, Miah S, Owen HC, Bryant H, Myers K, Larré S, Milo M, Rehman I, Rosario DJ, Di E et al (2009) Distinct microRNA alterations characterize high and low grade bladder cancer. *Can Res* 69: 8472–8481
- Chae YK, Ranganath K, Hammerman PS, Vaklavas C, Mohindra N, Kalyan A, Matsangou M, Costa R, Carneiro B, Villaflor VM et al (2017) Inhibition of the fibroblast growth factor receptor (FGFR) pathway: the current landscape and barriers to clinical application. *Oncotarget* 8: 16052–16074
- Chen S, Qiong Y, Gardner D (2005) A role for p38 mitogen-activated protein kinase and c-myc in endothelin-dependent rat aortic smooth muscle cell proliferation. *Hypertension* 47: 252–258
- Dang CV (2012) MYC on the path to cancer. *Cell* 149: 22–35
- Davarpanah NN, Yuno A, Trepel JB, Apolo AB (2017) Immunotherapy: a new treatment paradigm in bladder cancer. *Curr Opin Oncol* 29: 184
- Davies BR, Guan N, Logie A, Crafter C, Hanson L, Jacobs V, James N, Dudley P, Jacques K, Ladd B et al (2015) Tumors with AKT1E17K mutations are rational targets for single agent or combination therapy with AKT inhibitors. *Mol Cancer Ther* 14: 2441–2451
- Delmore JE, Issa GC, Lemieux ME, Rahl PB, Shi J, Jacobs HM, Kastiris E, Gilpatrick T, Paranal RM, Qi J et al (2011) BET bromodomain inhibition as a therapeutic strategy to target c-Myc. *Cell* 146: 904–917
- Earl J, Rico D, Carrillo-de-Santa-Pau E, Rodríguez-Santiago B, Méndez-Pertuz M, Auer H, Gómez G, Grossman HBHB, Pisano DGDG, Schulz WAWA et al (2015) The UBC-40 Urothelial Bladder Cancer cell line index: a genomic resource for functional studies. *BMC Genom* 16: 403
- El Behi M, Krumeich S, Lodillinsky C, Kamoun A, Tibaldi L, Sugano G, De Reynies A, Chapeaublanc E, Laplanche A, Lebret T et al (2013) An essential role for decorin in bladder cancer invasiveness. *EMBO Mol Med* 5: 1835–1851
- Flaherty KT, Infante JR, Daud A, Gonzalez R, Kefford RF, Sosman J, Hamid O, Schuchter L, Cebon J, Ibrahim N et al (2012) Combined BRAF and MEK inhibition in melanoma with BRAF V600 mutations. *N Engl J Med* 367: 1694–1703
- Fouquier J, Guedj M (2015) Analysis of drug combinations: current methodological landscape. *Pharmacol Res Perspect* 3: e00149
- Frey MR, Golovin A, Polk DB (2004) Epidermal growth factor-stimulated intestinal epithelial cell migration requires Src family kinase-dependent p38 MAPK signaling. *J Biol Chem* 279: 44513–44521
- Gregory MA, Qi Y, Hann SR (2003) Phosphorylation by glycogen synthase kinase-3 controls c-myc proteolysis and subnuclear localization. *J Biol Chem* 278: 51606–51612
- Haugsten EM, Wiedlocha A, Olsnes S, Wesche J (2010) Roles of fibroblast growth factor receptors in carcinogenesis. *Mol Cancer Res* 8: 1439–1452
- Hedegaard J, Lamy P, Nordentoft I, Algaba F, Hoyer S, Ulhøi BP, Vang S, Reinert T, Hermann GG, Mogensen K et al (2016) Comprehensive transcriptional analysis of early-stage urothelial carcinoma. *Cancer Cell* 30: 27–42
- Herrera-Abreu MT, Pearson A, Campbell J, Shnyder SD, Knowles MA, Ashworth A, Turner NC (2013) Parallel RNA interference screens identify EGFR activation as an escape mechanism in FGFR3-mutant cancer. *Cancer Discov* 3: 1058–1071
- Igea A, Nebreda AR (2015) The stress kinase p38 α as a target for cancer therapy. *Cancer Res* 75: 3997–4002
- Koul HK, Pal M, Koul S (2013) Role of p38 MAP kinase signal transduction in solid tumors. *Genes Cancer* 4: 342–359
- Kress TR, Sabo A, Amati B (2015) MYC: connecting selective transcriptional control to global RNA production. *Nat Rev Cancer* 15: 593–607
- Kurimchak AM, Shelton C, Duncan KE, Johnson KJ, Brown J, O'Brien S, Gabbasov R, Fink LS, Li Y, Lounsbury N, et al (2016) Resistance to BET bromodomain inhibitors is mediated by kinome reprogramming in ovarian cancer. *Cell Rep* 16: 1273–1286
- Leelahavanichkul K, Amornphimoltham P, Molinolo AA, Basile JR, Koontongkaew S, Gutkind JS (2014) A role for p38 MAPK in head and neck cancer cell growth and tumor-induced angiogenesis and lymphangiogenesis. *Mol Oncol* 8: 105–118
- Li F, Zhao C, Wang L (2014) Molecular-targeted agents combination therapy for cancer: developments and potentials. *Int J Cancer* 134: 1257–1269
- Li A, Shi D, Xu B, Wang J, Tang YL, Xiao W, Shen G, Deng W, Zhao C (2017) S100A6 promotes cell proliferation in human nasopharyngeal carcinoma via the p38/MAPK signaling pathway. *Mol Carcinog* 56: 972–984
- Lin CW, Lin JC, Prout GR (1985) Establishment and characterization of four human bladder tumor cell lines and sublines with different degrees of malignancy. *Cancer Res* 45: 5070–5079
- Liu H, Ai J, Shen A, Chen Y, Wang X, Peng X, Chen H, Shen Y, Huang M, Ding J et al (2016) c-Myc alteration determines the therapeutic response to FGFR inhibitors. *Clin Cancer Res* 23: 974–984
- Lovén J, Hoke HA, Lin CY, Lau A, David A, Vakoc CR, Bradner JE, Lee TI, Richard A (2013) Selective inhibition of tumor oncogenes by disruption of super-enhancers. *Cell* 153: 320–334
- Malchers F, Dietlein F, Schöttle J, Lu X, Nogova L, Albus K, Fernandez-Cuesta L, Heuckmann JM, Gautschi O, Diebold J et al (2014) Cell-autonomous and non-cell-autonomous mechanisms of transformation by amplified FGFR1 in lung cancer. *Cancer Discov* 4: 246–257
- Mertz JA, Conery AR, Bryant BM, Sandy P, Balasubramanian S, Mele DA, Bergeron L, Sims RJ III (2011) Targeting MYC dependence in cancer by inhibiting BET bromodomains. *Proc Natl Acad Sci USA* 108: 16669–16674
- Nakanishi Y, Akiyama N, Tsukaguchi T, Fujii T, Satoh Y, Ishii N, Aoki M (2015) Mechanism of oncogenic signal by the novel fusion kinase FGFR3-BAIAP2L1. *Mol Cancer Ther* 14: 704–712
- Niederst MJ, Engelman JA (2013) Bypass mechanisms of resistance to receptor tyrosine kinase inhibition in lung cancer. *Sci Signal* 6: re6
- Nishihara H, Hwang M, Kizaka-Kondoh S, Eckmann L, Insel PA (2004) Cyclic AMP promotes cAMP-responsive element-binding protein-dependent induction of cellular inhibitor of apoptosis protein-2 and suppresses apoptosis of colon cancer cells through ERK1/2 and p38 MAPK. *J Biol Chem* 279: 26176–26183
- Nogova L, Sequist LV, Perez Garcia JM, Andre F, Delord JP, Hidalgo M, Schellens JH, Cassier PA, Camidge DR, Schuler M et al (2017) Evaluation of BGJ398, a fibroblast growth factor receptor 1-3 kinase inhibitor, in patients with advanced solid tumors harboring genetic alterations in fibroblast growth factor receptors: results of a global phase I, dose-escalation and dose-expansion study. *J Clin Oncol* 35: 157–165
- van Oers JM, Lurkin I, van Exsel AJ, Nijssen Y, van Rhijn BW, van der Aa MN, Zwarthoff EC (2005) A simple and fast method for the simultaneous detection of nine fibroblast growth factor receptor 3 mutations in bladder cancer and voided urine. *Clin Cancer Res* 11: 7743–7748

- Posternak V, Cole MD (2016) Strategically targeting MYC in cancer. *F1000Res* 5: 408
- Powers CJ, McLeskey SW, Wellstein A (2000) Fibroblast growth factors, their receptors and signaling. *Endocr Relat Cancer* 7: 165–197
- Powles T, Eder JP, Fine GD, Braiteh FS, Loria Y, Cruz C, Bellmunt J, Burris HA, Petrylak DP, Teng S-L et al (2014) MPDL3280A (anti-PD-L1) treatment leads to clinical activity in metastatic bladder cancer. *Nature* 515: 558–562
- Qiu WH, Zhou BS, Chu PG, Chen WG, Chung C, Shih J, Hwu P, Yeh C, Lopez R, Yen Y (2005) Over-expression of fibroblast growth factor receptor 3 in human hepatocellular carcinoma. *World J Gastroenterol* 11: 5266–5272
- Ran L, Sirota I, Cao Z, Murphy D, Chen Y, Shukla S, Xie Y, Kaufmann MC, Gao D, Zhu S et al (2015) Combined inhibition of MAP Kinase and KIT signaling synergistically destabilizes ETV1 and suppresses GIST tumor growth. *Cancer Discov* 5: 304–315
- Rebouissou S, Bernard-Pierrot I, de Reyniès A, Lepage M-L, Krucker C, Chapeaublanc E, Héroult A, Kamoun A, Caillault A, Letouzé E et al (2014) EGFR as a potential therapeutic target for a subset of muscle-invasive bladder cancers presenting a basal-like phenotype. *Sci Transl Med* 6: 244ra291
- Ritchie ME, Phipson B, Wu D, Hu Y, Law CW, Shi W, Smyth GK (2015) limma powers differential expression analyses for RNA-sequencing and microarray studies. *Nucleic Acids Res* 43: e47
- Rouanne M, Loria Y, Lebret T, Soria JC (2016) Novel therapeutic targets in advanced urothelial carcinoma. *Crit Rev Oncol Hematol* 98: 106–115
- Sears R, Nuckolls F, Haura E, Taya Y, Tamai K, Nevins JR (2000) Multiple Ras-dependent phosphorylation pathways regulate Myc protein stability. *Genes Dev* 14: 2501–2514
- Shu S, Lin CY, He HH, Witwicki RM, Tabassum DP, Roberts JM, Janiszewska M, Hun JS, Yi L, Ryan J et al (2016) Response and resistance to BET bromodomain inhibitors in triple negative breast cancer. *Nature* 67: 413–417
- Singh D, Chan JM, Zoppoli P, Niola F, Castano A, Liu EM, Reichel J, Poratti P, Qiu K, Gao Z et al (2012) Transforming fusions of FGFR and TACC genes in human glioblastoma. *Science* 337: 1231–1235
- Stine ZE, Walton ZE, Altam BJ, Hsieh AL, Dang CV (2015) MYC, metabolism and cancer. *Cancer Discov* 312: 2668–2675
- Tcga (2014) Comprehensive molecular characterization of urothelial bladder carcinoma. *Nature* 507: 315–322
- Tomlinson DC, Knowles MA, Speirs V (2012) Mechanisms of FGFR3 actions in endocrine resistant breast cancer. *Int J Cancer* 130: 2857–2866
- Tsai W-B, Aiba I, Long Y, Lin H-K, Feun L, Savaraj N, Kuo TM (2012) Activation of Ras/PI3K/ERK pathway induces c-Myc stabilization to upregulate argininosuccinate synthetase, leading to arginine deiminase resistance in melanoma cells. *Can Res* 29: 997–1003
- Vivanco I, Sawyers CL (2002) The phosphatidylinositol 3-Kinase AKT pathway in human cancer. *Nat Rev Cancer* 2: 489–501
- Wada M, Canals D, Adada M, Coant N, Salama MF, Helke KL, Arthur JS, Shroyer KR, Kitatani K, Obeid LM et al (2017) P38 delta MAPK promotes breast cancer progression and lung metastasis by enhancing cell proliferation and cell detachment. *Oncogene* 36: 6649–6657
- Walz S, Lorenzin F, Morton J, Wiese KE, von Eyss B, Herold S, Rycak L, Dumay-Odelot H, Karim S, Bartkuhn M et al (2014) Activation and repression by oncogenic MYC shape tumour-specific gene expression profiles. *Nature* 511: 483–487
- Wang J, Mikse O, Liao RG, Li Y, Tan L, Janne PA, Gray NS, Wong KK, Hammerman PS (2015) Ligand-associated ERBB2/3 activation confers acquired resistance to FGFR inhibition in FGFR3-dependent cancer cells. *Oncogene* 34: 2167–2177
- Wang L, Sustic T, Leite de Oliveira R, Liefink C, Halonen P, van de Ven M, Beijersbergen RL, van den Heuvel MM, Bernards R, van der Heijden MS (2017) A functional genetic screen identifies the phosphoinositide 3-kinase pathway as a determinant of resistance to fibroblast growth factor receptor inhibitors in FGFR mutant urothelial cell carcinoma. *Eur Urol* 71: 858–862
- Williams SV, Hurst CD, Knowles MA (2013) Oncogenic FGFR3 gene fusions in bladder cancer. *Hum Mol Genet* 22: 795–803
- Witjes JA, Palou J, Soloway M, Lamm D, Kamat AM, Brausi M, Persad R, Buckley R, Colombel M, Bohle A (2013) Current clinical practice gaps in the treatment of intermediate- and high-risk non-muscle-invasive bladder cancer (NMIBC) with emphasis on the use of bacillus Calmette-Guerin (BCG): results of an international individual patient data survey (IPDS). *BJU Int* 112: 742–750
- Wu Y-M, Su F, Kalyana-Sundaram S, Khazanov N, Cao X, Lonigro RJ, Vats P, Wang R, Lin S-F, Cheng A-J et al (2013) Identification of targetable FGFR gene fusions in diverse cancers. *Cancer Discov* 3: 636–647
- Yeh E, Cunningham M, Arnold H, Chasse D, Monteith T, Ivaldi G, Hahn WC, Stukenberg PT, Shenolikar S, Uchida T et al (2004) A signalling pathway controlling c-Myc degradation that impacts oncogenic transformation of human cells. *Nat Cell Biol* 6: 308–318



License: This is an open access article under the terms of the Creative Commons Attribution 4.0 License, which permits use, distribution and reproduction in any medium, provided the original work is properly cited.